

Randomized measurements for multi-parameter quantum metrology

Sisi Zhou^{1,2,*} and Senrui Chen^{3,4,†}

¹*Perimeter Institute for Theoretical Physics, Waterloo, Ontario N2L 2Y5, Canada*

²*Department of Physics and Astronomy, Department of Applied Mathematics and Institute for Quantum Computing, University of Waterloo, Ontario N2L 2Y5, Canada*

³*Pritzker School of Molecular Engineering, The University of Chicago, Chicago, Illinois 60637, USA*

⁴*Institute for Quantum Information and Matter, California Institute of Technology, Pasadena, CA 91125, USA*

(Dated: January 16, 2026)

The optimal quantum measurements for estimating different unknown parameters in a parameterized quantum state are usually incompatible with each other. Traditional approaches to addressing the measurement incompatibility issue, such as the Holevo Cramér–Rao bound, suffer from multiple difficulties towards practical applicability, as the optimal measurement strategies are usually state-dependent, difficult to implement and also take complex analyses to determine. Here we study randomized measurements as a new approach for multi-parameter quantum metrology. We show quantum measurements on single copies of quantum states given by 3-designs perform near-optimally when estimating an arbitrary number of parameters in pure states and more generally, approximately low-rank well-conditioned states, whose metrological information is largely concentrated in a low-dimensional subspace. The near-optimality is also shown in estimating the maximal number of parameters for three types of mixed states that are well-conditioned on their supports. Examples of fidelity estimation and Hamiltonian estimation are explicitly provided to demonstrate the power and limitation of randomized measurements in multi-parameter quantum metrology.

I. INTRODUCTION

Quantum metrology is the study of parameter estimation in quantum systems [1–4]. It has extensive applications in optical interferometry [5–8], frequency detection [9–18] and quantum imaging [19–22], etc. In single-parameter estimation, the quantum Cramér–Rao bound (QCRB) characterizes the ultimate precision limit of estimating one parameter in quantum states through an information-theoretic quantity called the quantum Fisher information (QFI) [23–29], which is the classical Fisher information (CFI) maximized over all possible quantum measurements on quantum states. In multi-parameter estimation, however, the quantum Fisher information matrix (QFIM) and the corresponding quantum Cramér–Rao bound is not always attainable because the optimal quantum measurements that correspond to different parameters may not commute and thus cannot be simultaneously implemented. Trade-offs among the estimation precisions for different parameters must be taken into consideration [30–60].

One popular solution of the measurement incompatibility issue in multi-parameter metrology is to minimize the weighted sum of estimation variances for a given cost matrix, instead of aiming at optimizing the estimation variances for all parameters. Holevo’s version of the quantum Cramér–Rao bound (HCRB) [26, 39–41], which provides a tight lower bound for the weighted sum, was extensively researched and applied [34, 35, 61–66]. It is numerically solvable through semidefinite programs [61

and analytically solvable when the number of parameters is two [64]. The HCRB is attainable for generic quantum states using collective measurements on infinitely many copies of quantum states [39–41]. When restricted to individual measurements on single copies of states, the HCRB is attainable for pure states [31]. Individual measurements also have known solutions for some specific families of states, such as single-qubit states, via other numerically solvable bounds (e.g., the Nagaoka–Hayashi bound [32, 33] and the Gill–Massar bound [30]). Another line of research in multi-parameter estimation focuses on local state tomography, where optimal measurements for uniformly estimating all parameters in pure states called Fisher-symmetric measurements were found and studied [47–49].

Despite the success of previous efforts in addressing multi-parameter estimation problems in quantum metrology, several obstacles exist against its practical usefulness, in particular when the *system dimension* is large. The first obstacle is the *implementation complexity*. Collective measurements on a large number of states are required in general, which are almost experimentally infeasible. In situations where individual measurements are sufficient [31–33, 47–49], the implementation can still be challenging when the measurement basis is complex. The second obstacle is the *computational resource* required for identifying the optimal measurements. The numerical computation of the HCRB scales polynomially with respect to the system dimension, which can become quickly intractable e.g., for multi-qubit systems as the number of qubits increases. Note that searching for optimal individual measurements that minimize the weighted sum of estimation variance is an NP-hard problem that involves minimization over a separable cone [65] which is even

* sisi.zhou26@gmail.com

† csenrui@gmail.com

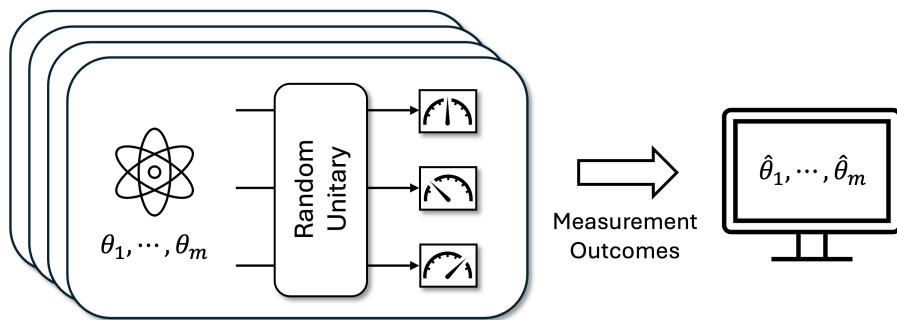


Figure 1. Schematics of randomized measurements for multi-parameter quantum metrology. The measurement is taken on *individual* copies of the same parameterized state $\rho_\theta := \rho_{\theta_1, \dots, \theta_m}$. The goal is to obtain estimates $\hat{\theta} = (\hat{\theta}_1, \dots, \hat{\theta}_m)$ with the highest precision as the number of copies approaches infinity. In all of our theorems showing the near-optimality of randomized measurements, it suffices to take the measurement to be a 3-design.

	Traditional approaches	3-design measurements
Computational complexity (for finding measurements)	Usually at least polynomial in system dimension	None (state-independent)
Implementation complexity	Usually unknown (polynomial in system dimension)	Polynomial in qubit number

Table I. Comparison of traditional (individual) measurement protocols and our randomized measurement protocol for multi-parameter quantum metrology. See [Appx. A](#) for detailed explanations and extended discussions on collective measurements.

more challenging. Finally, the optimal quantum measurements obtained from traditional approaches usually depend on the quantum state, meaning they need to be updated adaptively as the prior knowledge of the state is refined during the experiment. The optimal measurements can also depend on the cost matrix, limiting its application scenarios, e.g., in situations where the cost matrix is revealed only in the post-processing phase after the measurement [67].

Here we propose randomized measurement protocols for multi-parameter metrology, where the above mentioned obstacles are alleviated (see [Table I](#)). Random unitaries and measurements [68] are widely applied in quantum device benchmarking [69–71], learning and tomography [67, 72, 73], etc., but were rarely explored in multi-parameter quantum metrology. Below we mostly focus on randomized measurements on individual copies of quantum states whose measurement basis forms a (complex projective) 3-design [74, 75], which can be realized through applying a unitary 3-design [70, 76, 77] prior to a projection onto the computational basis. The implementation of 3-designs was thoroughly investigated in previous literature. In multi-qubit systems, random Clifford circuits form a unitary 3-design [78–80] and can be efficiently implemented through linear-depth quantum circuits in 1D architecture [81, 82] and log-depth circuits in all-to-all connected architecture with ancilla [83, 84]. For general qudit systems, approximate implementations [85–88] and explicit constructions [89–91] were also proposed.

In this work, we demonstrate the optimality of randomized measurements for different families of quantum

states (see [Table II](#)). We first prove the near-optimality of randomized measurements for multi-parameter pure state estimation. We show the classical Fisher information matrix (CFIM) obtained from randomized measurements attains the QFIM up to a constant factor no larger than 4 for any parameterized pure states in any finite-size systems. Next, we consider approximately low-rank well-conditioned states, which are states whose metrological information is largely concentrated in a low-dimensional subspace, and further demonstrate the saturation of the QFIM up to a constant factor, extending the result of pure states. For both pure states and approximately low-rank well-conditioned states, the near-optimality is independent of the choice of cost matrices, aligning with the “measure first, ask questions later” framework [67]. We also investigate mixed states in general, and show the near-optimality of randomized measurements for three families of quantum mixed states which have a maximal number of unknown parameters. Near-optimality is proved when the cost matrix is the QFIM, a metric that was commonly used to guarantee invariance under reparameterization and equal importance of all parameters [30, 47, 48]. Finally, we provide examples, including fidelity estimation and Hamiltonian estimation (with and without quantum noise), demonstrating the applicability and limitation of randomized measurements for different quantum metrological tasks. In particular, we provide a mixed state fidelity estimation example where randomized measurements do not perform nearly optimally. Apart from theoretical results, we numerically implement a pure state fidelity estimation example using randomized measurements and a newly-designed near-optimal esti-

Families of Parameterized States	Randomized Measurements	Examples
Pure states (Sec. IV)	Near-optimal (Theorem 1)	Sec. VII A, Sec. VIIC 1
Approximately low-rank well-conditioned states (Sec. V)	Near-optimal (Theorem 2, Theorem 3)	Sec. VIIC 2
Full-parameter rank- r well-conditioned states (Sec. VI)	Weakly near-optimal (Theorem 4)	-
General mixed states	Not always (weakly) near-optimal	Sec. II, Sec. VIIB

Table II. Summary of main results.

mator, validating our theory and demonstrating a clear advantage over existing protocols (Fig. 3). These results highlight randomized measurements as a powerful tool for multi-parameter quantum metrology with the potential for broad applications.

II. INFORMAL OVERVIEW

Below we first briefly introduce the setting of multi-parameter quantum metrology (a more formal introduction is deferred to Sec. III A) and then we provide an informal overview of our results, with a focus on explaining the underlying intuition behind them.

Consider a d -dimensional parameterized quantum state ρ_θ in Hilbert space \mathcal{H} , where parameters are denoted by $\theta = (\theta_1, \theta_2, \dots, \theta_m)$. m is the number of parameters and $\Theta \subseteq \mathbb{R}^m$ is the domain of θ . An estimator $\hat{\theta}(x)$ and the corresponding positive operator-valued measurement (POVM) $M = \{M_x\}_x$ is a function that maps the measurement outcomes x to Θ . Here M_x are positive semidefinite measurement operators satisfying $\sum_x M_x = \mathbb{1}$. The performance of an estimator at θ is characterized by the *mean squared error matrix* (MSEM)

$$V(M, \hat{\theta})_{ij} = \sum_x (\hat{\theta}(x)_i - \theta_i)(\hat{\theta}(x)_j - \theta_j) \text{Tr}(\rho_\theta M_x). \quad (1)$$

For single-parameter estimation (i.e., $m = 1$), V is a scalar called the mean squared error (MSE).

In the paradigm of local parameter estimation, we focus on analyzing the performance of *locally unbiased estimators* that are unbiased at the true value of θ and in its vicinity up to the first order. It is relevant in metrological situations where the prior knowledge of θ is already given in the vicinity of its true value, or roughly obtained from a pre-estimation phase (which usually consumes a number of experiments that are negligible compared to N , the total number of copies of states available) [30, 41, 92–96].

The Cramér–Rao bound (CRB) [92–96] states that for any locally unbiased estimator at θ ,

$$V(M, \hat{\theta}) \succeq I(M)^{-1}, \quad (2)$$

where $A \succeq B$ denotes a relationship between two positive semidefinite matrices A and B where $A - B$ is positive semidefinite. Note that here we use “ \succeq ” instead of “ \geq ” to emphasize the objects under comparison are matrices, while later on when the discussion is restricted to single-parameter estimation and $I(M)$ and J become scalars,

we will use \geq instead. $I(M)$ is the classical Fisher information matrix (CFIM), defined by

$$I(M)_{ij} = \sum_{x, p_x := \text{Tr}(\rho_\theta M_x) \neq 0} \frac{1}{p_x} \frac{\partial p_x}{\partial \theta_i} \frac{\partial p_x}{\partial \theta_j}. \quad (3)$$

$I(M)$ is a function of the POVM and ρ_θ , and is independent of the estimators. The quantum Cramér–Rao bound (QCRB) [23–29] further states that, for any locally unbiased estimator at θ ,

$$V(M, \hat{\theta}) \succeq I(M)^{-1} \succeq J^{-1}, \quad (4)$$

where J is the quantum Fisher information matrix (QFIM) as a function of ρ_θ . For single-parameter estimation, the quantum Fisher information (QFI) J is equal to the classical Fisher information (CFI) $I(M)$ maximized over all POVMs [27]. For multi-parameter estimation, however, this does not always hold. The reason is the measurements that are optimal with respect to different parameters may not be compatible with each other, i.e., cannot be implemented simultaneously.

Since the CFIM in general cannot attain the QFIM, we introduce the concept of *near-optimality* (see details in Sec. III C) and investigate situations where near-optimal measurements exist. It is a property of a family of POVMs, with a corresponding state family, stating that the ratio between the CFIM and the QFIM is bounded below by a constant.

We find in Theorem 1 that 3-design measurements are near-optimal for pure states. A simple example below provides some intuition behind this result. Consider a one-qubit pure state $|\psi_\theta\rangle = \frac{|0\rangle + e^{i\theta}|1\rangle}{\sqrt{2}}$ with one unknown parameter θ . The optimal choice of measurement basis will be in the x - y plane of the Bloch sphere (see Fig. 2) because any component in the z axis is not useful in discriminating $|\psi_\theta\rangle$ and $|\psi_{\theta+d\theta}\rangle$. Consider a projective measurement onto basis $\{\frac{|0\rangle \pm e^{i\beta}|1\rangle}{\sqrt{2}}\}$. The corresponding probability distribution is $\{\cos^2(\frac{\beta-\theta}{2}), \sin^2(\frac{\beta-\theta}{2})\}$, and the CFI

$$\begin{aligned} I(M) &= \frac{(\partial_\theta(\sin^2(\frac{\beta-\theta}{2})))^2}{\cos^2(\frac{\beta-\theta}{2})} + \frac{(\partial_\theta(\cos^2(\frac{\beta-\theta}{2})))^2}{\sin^2(\frac{\beta-\theta}{2})} \\ &= \sin^2\left(\frac{\beta-\theta}{2}\right) + \cos^2\left(\frac{\beta-\theta}{2}\right) = 1. \end{aligned}$$

In fact, the CFI is $I(M) = J = 1$ for any $\beta - \theta \notin \frac{\pi}{2}\mathbb{Z}$, which means (almost) all projective measurements on the

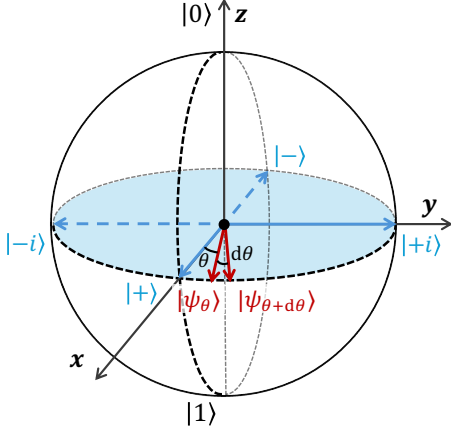


Figure 2. Bloch sphere. Any projective measurement onto the basis in the x - y plane is optimal in the task of estimating parameter θ in $|\psi_\theta\rangle = \frac{|0\rangle + e^{i\theta}|1\rangle}{\sqrt{2}}$, including the x -basis $\{|\pm\rangle = \frac{|0\rangle \pm |1\rangle}{\sqrt{2}}\}$ and the y -basis $\{|\pm i\rangle = \frac{|0\rangle \pm i|1\rangle}{\sqrt{2}}\}$.

x - y plane of the Bloch sphere can achieve the QFI. To intuitively understand why all measurements on the x - y plane can yield the same performance, we consider the situation when θ is a small positive angle (see Fig. 2) and compare projective measurements onto $|\pm\rangle$ (eigenstates of Pauli- X , $\beta = 0$) and $|\pm i\rangle$ (eigenstates of Pauli- Y , $\beta = \frac{\pi}{2}$). The probabilities of obtaining $|+\rangle$ and $|-\rangle$ as outcomes are approximately $1 - \theta^2/4$ and $\theta^2/4$, respectively, with corresponding derivatives approximately $\mp\theta/2$. On the other hand, for a measurement in the $|\pm i\rangle$, $|\pm i\rangle$ basis, the outcome probabilities are approximately $1/2 \mp \theta/2$, with derivatives around $\mp 1/2$. In the first case, the derivatives of the probabilities are small, but the distribution is highly sensitive to changes in their values. In the second case, the derivatives are large, but the distribution is less sensitive to changes in the values of probabilities. These two factors affect the overall estimation precision in opposing ways, ultimately balancing each other out. As a result, the CFI remains the same across all measurements in the x - y plane. This shows for pure states the optimal measurement to estimate one parameter is not unique and can spread extensively in the entire space of POVMs, which provides evidence that randomized measurements may be able to achieve a near-optimal performance.

To see why the above discussion is still (surprisingly) meaningful in a general d -dimensional Hilbert space, we perform the following hand-wavy analysis on the scaling of the CFI with respect to d . Consider a d -dimensional pure state $|\psi_\theta\rangle$ and a projective measurement $M = \{U|x\rangle\langle x|U^\dagger\}_{x=1}^d$ where $|x\rangle$ is the computational basis in the Hilbert space \mathcal{H} . The CFI

$$I(M) = \sum_x \frac{\langle x|U^\dagger(|\partial_\theta\psi_\theta\rangle\langle\psi_\theta| + |\psi_\theta\rangle\langle\partial_\theta\psi_\theta|)U|x\rangle^2}{\langle x|U^\dagger|\psi_\theta\rangle\langle\psi_\theta|U|x\rangle}.$$

We can naively compute the expectation values of the denominators and the numerators when U is sampled from the Haar measure. We have

$$\mathbb{E}_U[\langle x|U^\dagger|\psi_\theta\rangle\langle\psi_\theta|U|x\rangle] = \frac{1}{d},$$

$$\mathbb{E}_U[\langle x|U^\dagger(|\partial_\theta\psi_\theta\rangle\langle\psi_\theta| + |\psi_\theta\rangle\langle\partial_\theta\psi_\theta|)U|x\rangle^2] = \frac{J}{2d(d+1)},$$

where we use the property of 2-design (see Eq. (31)) and the fact that the pure-state QFI is $J = 4(\langle\partial_\theta\psi|\partial_\theta\psi\rangle - \langle\psi|\partial_\theta\psi\rangle\langle\partial_\theta\psi|\psi\rangle)$. If naively, in the expression of $I(M)$, we replace all numerators and denominators with their expectation values, we can see the ratio between $I(M)$ and J is a constant independent of d . Roughly speaking, as d increases, the derivative of each probability decreases, but the distribution also becomes more sensitive to changes in the values of probabilities—because the number of possible outcomes also increases. For example, compare a Bernoulli distribution $\{1 - \theta, \theta\}$ to a $(d+1)$ -outcome probability distribution $\{1 - \theta, \theta/d, \dots, \theta/d\}$. Their CFIs with respect to θ are the same, equal to $1/(\theta(1 - \theta))$, and the latter has more numbers of outcomes but smaller derivatives of each probability. In our case, these two factors also balance each other out, keeping the ratio between $I(M)$ and J a constant. As the structure of the randomized measurements does not depend on the specific choice of parameter, the result should extend naturally to multi-parameter estimation.

The above analysis, though not rigorous, indicates when a measurement is sufficiently random, it may potentially achieve near-optimality for pure state estimation. We prove this rigorously in Theorem 1 for 3-design measurements where we explicitly construct a locally unbiased estimator that achieves the QFIM up to a constant. We further generalize this result to Theorem 2 and Theorem 3, where we show near-optimality for approximately low-rank well-conditioned states. Here, *approximately low-rank well-conditioned states* means states which have a low-rank support on which eigenvalues are above a positive constant and the QFIM is close to the QFIM of the entire state. It is practically relevant, e.g., in situations when we estimate parameters in pure states or low-rank states subject to weak noise.

We can perform a similar dimension analysis to understand the intuition behind this result. Consider a rank- r state $\rho_\theta = \frac{1}{r}\Pi$ where Π is a projector and $\partial_\theta\rho_\theta = -i[H, \rho_\theta]$. Then calculation shows the QFI

$$J = \frac{4}{r}\text{Tr}(H\Pi H\Pi^\perp), \quad (5)$$

where $\Pi^\perp = \mathbb{1} - \Pi$. For $M = \{U|x\rangle\langle x|U^\dagger\}_{x=1}^d$,

$$I(M) = \sum_x \frac{\langle x|U^\dagger(\frac{1}{r}(H\Pi - \Pi H))U|x\rangle^2}{\langle x|\frac{1}{r}\Pi|x\rangle}.$$

For randomized U that is at least 2-design, the average values of the denominators and the numerators are

$$\mathbb{E}_U[\langle x|U^\dagger\left(\frac{1}{r}\Pi\right)U|x\rangle] = \frac{1}{d},$$

$$\mathbb{E}_U[\langle x|U^\dagger\left(\frac{1}{r}(H\Pi - \Pi H)\right)U|x\rangle^2] = \frac{J}{2r^2d(d+1)}.$$

When r is a constant, i.e., ρ_θ is low-rank, we can see the ratio between $I(M)$ and J is also a constant independent of d —if we naively replace all numerators and denominators with their expectation values in the expression of $I(M)$. Although the replacement is not mathematically valid, it provides some intuition behind [Theorem 2](#) and [Theorem 3](#).

One key assumption in the above definition of approximately low-rank well-conditioned states is all eigenvalues in its low-rank support must be above a positive constant, the following shows a *counter example* where this assumption is violated and randomized measurements are not near-optimal. Rigorous discussions can be found in [Sec. VII B](#). Consider a single-qubit state $\rho_f = f|0\rangle\langle 0| + (1-f)|1\rangle\langle 1|$ where f is to be estimated. The optimal measurement is $M = \{|0\rangle\langle 0|, |1\rangle\langle 1|\}$ that achieves $I(M) = J = 1/(f(1-f))$. When f or $1-f$ is sufficiently small, J can be arbitrarily large. On the other hand, if we consider measurement $M = \{U|0\rangle\langle 0|U^\dagger, U|1\rangle\langle 1|U^\dagger\}$, we have

$$I(M) = \sum_{x=0,1} \frac{\langle x|U^\dagger(|0\rangle\langle 0| - |1\rangle\langle 1|)U|x\rangle^2}{\langle x|(f|0\rangle\langle 0| + (1-f)|1\rangle\langle 1|)|x\rangle},$$

and for randomized U in the 2-dimensional Hilbert space (that is at least 2-design),

$$\begin{aligned} \mathbb{E}_U[\langle x|(f|0\rangle\langle 0| + (1-f)|1\rangle\langle 1|)|x\rangle] &= \frac{1}{2}, \\ \mathbb{E}_U[\langle x|U^\dagger(|0\rangle\langle 0| - |1\rangle\langle 1|)U|x\rangle^2] &= \frac{2}{3}, \end{aligned}$$

both of which are independent of f . It suggests that as $f \rightarrow 0$, the CFI of randomized measurements will not approach infinity—thus an infinitely large gap exists between the CFI and the QFI. In particular, the counter example is a qubit estimation example, which means even for states constrained in a finite-dimensional space, randomized measurements cannot be always near-optimal.

For general mixed states, not only randomized measurements cannot be near-optimal, near-optimal measurements (that only acts on individual copies of quantum states) might not exist at all. A typical example is the full tomography of mixed states, where the measurement incompatibility issue cannot be avoided unless measurements on many copies of states are allowed—which is beyond the discussion of our work. Thus, we introduce the concept of *weak near-optimality* to describe measurements that perform almost the best among all other individual measurements using a natural figure of merit as detailed in [Sec. III C](#). We found in [Theorem 4](#) that 3-design measurements are weakly near-optimal when estimating all parameters describing a rank- r state that is well-conditioned on its support—we call this the estimation of *full-parameter* rank- r well-conditioned states. Our result is consistent with other existing results in the

field of state tomography—e.g., Clifford measurements are optimal for learning all Pauli observables of general mixed states [[72](#), [97](#)].

When m , the number of parameters to be estimated in general mixed states, is not maximal, randomized measurements are usually not weakly near-optimal. One typical situation is when the QFIM is attainable because the optimal POVMs with respect to different parameters commute. For example, we can consider an n -qubit state

$$\rho_\theta = \frac{\mathbb{1} + \sum_{i \in \mathcal{S}^\circ} \theta_i P_i}{2^n}, \quad (6)$$

where \mathcal{S}° is a stabilizer group [[98](#)] excluding $\mathbb{1}$ and we consider parameter estimation at $\theta_i = 0$. The number of parameters $m = 2^n - 1$ (which is far from the maximal number of parameters $4^n - 1$), the QFIM $J_{ij} = \delta_{ij}$ is achievable by projective measurement onto the common eigenstates of the stabilizer group. On the other hand, consider a randomized measurement $M = \{p_U U|x\rangle\langle x|U^\dagger\}_{x,U}$ where $|x\rangle$ is the computational basis and $\{p_U, U\}$ is a unitary 2-design, we have

$$I(M)_{ij} = \sum_{U,x} p_U \langle x|U^\dagger P_i U|x\rangle \langle x|U^\dagger P_j U|x\rangle = \frac{\delta_{ij}}{2^n + 1}, \quad (7)$$

which is a factor $1/(2^n + 1)$ away from optimal. In general, it is open for which types of mixed states randomized measurements are weakly near-optimal.

Below, we will review concepts in multi-parameter quantum metrology and some previous results in [Sec. III](#). We provide the exact statements and proofs of our theorems in [Sec. IV–Sec. VI](#). In [Sec. VII](#), we consider specific examples where we show how to apply our result in estimating fidelity of pure states and in Hamiltonian estimation, and also prove rigorously randomized measurements are not near-optimal when estimating fidelity of some types of mixed states.

III. PRELIMINARIES

A. Multi-parameter estimation

Here we provide a detailed overview of multi-parameter estimation. First, an estimator $(\hat{\theta}, M)$ is called *locally unbiased* at $\theta = \theta^0$ if and only if

$$\theta^0 = \sum_x \hat{\theta}(x) \text{Tr}(\rho_\theta M_x) \Big|_{\theta=\theta^0}, \quad (8)$$

$$\delta_{ij} = \frac{\partial}{\partial \theta_i} \sum_x \hat{\theta}_j(x) \text{Tr}(\rho_\theta M_x) \Big|_{\theta=\theta^0}, \quad \forall i, j. \quad (9)$$

Throughout this paper, when there is no ambiguity, we will usually not distinguish between θ^0 and θ , and assume all functions are evaluated at θ for notation simplicity. We will only explicitly use the notation θ^0 when we need

to distinguish between the local point θ^0 and the true unknown parameter, which will be denoted by θ .

In classical statistics, the MSEM of any locally unbiased estimator at θ is bounded below by the inverse of the CFIM (see Eq. (2)). $I(M)$ is a positive semidefinite matrix in $\mathbb{R}^{m \times m}$ and we further assume in this work that $I(M)$ is strictly positive, which means each parameter is identifiable (unless stated otherwise). This forbids redundant parameterization and puts an upper bound on the number of allowed parameters. Note that $I(M)$ depends on the state ρ_θ and the value of θ but they are omitted for simplicity, as is the case with many other concepts defined below. The CRB at θ^0 is saturable via the following locally unbiased estimator [92–96] defined by

$$\hat{\theta}_i^{\text{opt}}(y; \theta^0) = \theta_i^0 + \sum_x (\alpha_{i,x} |_{\theta=\theta^0}) \hat{p}_x(y), \quad (10)$$

where $(\cdot; \star)$ indicates dependence on \star , $\alpha_{i,x} = \sum_j (I(M)^{-1})_{ij} \frac{\partial_j p_x}{p_x}$ and ∂_i is used as a shorthand for $\frac{\partial}{\partial \theta_i}$. $\hat{p}_x(y) = \delta_{xy}$ where y is the measurement outcome. $\mathbb{E}[\hat{p}_x] = p_x = \text{Tr}(\rho_\theta M_x)$ and $\mathbb{E}[\hat{p}_x \hat{p}_y] = \delta_{xy} p_x$. It achieves the CRB, i.e.,

$$V(M, \hat{\theta}^{\text{opt}}) = I(M)^{-1}. \quad (11)$$

Given N copies of ρ_θ , the CRB is asymptotically saturable for large N using the (asymptotically unbiased) maximum likelihood estimator $\hat{\theta}_{\text{MLE}}^{(N)}$ [92–96]— $\sqrt{N}(\hat{\theta}_{\text{MLE}}^{(N)} - \theta)$ converges in distribution to a normal distribution centered around 0 with variance equal to $I(M)^{-1}$ as $N \rightarrow \infty$. Note that $I(M)$ here is additive— $I(M^{\otimes N}) = NI(M)$, where we use $I(M^{\otimes N})$ to denote the CFIM when measuring $\rho_\theta^{\otimes N}$ using POVM $M^{\otimes N} = \{\otimes_{i=1}^N M_{x_i}\}_{(x_1, x_2, \dots, x_N)}$. The factor of N naturally occurs from the classical central limit theorem, where the estimation variance is improved by a factor of N when N i.i.d. samples are taken.

The CRB is a purely classical result. It provides a lower bound on $V(M, \hat{\theta})$ that depends on the choice of POVM. The QCRB [23–29] (see Eq. (4)) provides a more general lower bound when the POVM can be chosen freely. J is the QFIM as a function of ρ_θ and is additive with respect to ρ_θ . It is defined by

$$J_{ij} = \frac{1}{2} \text{Tr}(\rho_\theta \{L_i, L_j\}), \quad (12)$$

where $\{\cdot, \cdot\}$ is the anti-commutator and L_i are Hermitian operators called symmetric logarithmic derivative (SLD) operators, defined through

$$\frac{\partial \rho_\theta}{\partial \theta_i} = \frac{1}{2} (L_i \rho_\theta + \rho_\theta L_i). \quad (13)$$

L_i is not uniquely defined by the equation above, but J is invariant under different choices of L_i . In this work,

we fix the definition of L_i as below for future use.

$$L_i := 2 \sum_{jk, \lambda_j + \lambda_k > 0} \frac{\langle \psi_j | \partial_i \rho_\theta | \psi_k \rangle}{\lambda_j + \lambda_k} |\psi_j\rangle \langle \psi_k|, \quad (14)$$

where $\sum_j \lambda_j |\psi_j\rangle \langle \psi_j| = \rho_\theta$ is the spectral decomposition of ρ_θ . The QFIM J can be calculated as

$$J_{ij} = 2 \sum_{k\ell, \lambda_k + \lambda_\ell > 0} \frac{\text{Re}[\langle \psi_k | \partial_i \rho_\theta | \psi_\ell \rangle \langle \psi_\ell | \partial_j \rho_\theta | \psi_k \rangle]}{\lambda_k + \lambda_\ell}. \quad (15)$$

For single-parameter estimation, i.e., when $m = 1$, J and $I(M)$ are scalars, and J is attainable [27]:

$$J = \max_{M: \text{POVM}} I(M). \quad (16)$$

Therefore, the QCRB (Eq. (4)) is asymptotically attainable, making the QFI J a perfect figure of merit to characterize the performance of local parameter estimation on state ρ_θ . For multi-parameter estimation, however, J may not be attainable by any POVM due to the measurement incompatibility issue.

B. Previous Results

1. Holevo Cramér–Rao bound

To address the measurement incompatibility issue, it helps to consider minimization of the *weighted mean squared error* (WMSE), $\text{Tr}(WV(M, \hat{\theta}))$, where W is a cost matrix that is positive semidefinite in $\mathbb{R}^{m \times m}$. The QCRB automatically provides a lower bound on the WMSE,

$$\text{Tr}(WV(M, \hat{\theta})) \geq \text{Tr}(WJ^{-1}) =: C_F(W). \quad (17)$$

The HCRB [26, 39–41] provides a tighter lower bound which states

$$\text{Tr}(WV(M, \hat{\theta})) \geq C_H(W) := \min_{\mathbf{X} := \{X_i\}_i} \text{Tr}(W \text{Re}[Z(\mathbf{X})]) + \left\| \sqrt{W} \text{Im}[Z(\mathbf{X})] \sqrt{W} \right\|_1, \quad (18)$$

where X_i are Hermitian operators acting on \mathcal{H} satisfying $\text{Tr}(X_i \partial_j \rho_\theta) = \delta_{ij}$ and $Z(\mathbf{X})_{ij} = \text{Tr}(\rho_\theta X_i X_j)$. Both $C_F(W)$ and $C_H(W)$ are additive with respect to ρ_θ . The HCRB is asymptotically approachable through a sequence of *collective measurements* $M^{(N)}$ acting on $\rho_\theta^{\otimes N}$ when the state and estimators satisfy certain regularity conditions [39–41]. The HCRB is computable through semidefinite programming [61] and can be approximated by the QCRB up to a factor of two as [51, 63]

$$C_F(W) \leq C_H(W) \leq 2C_F(W). \quad (19)$$

The HCRB is achievable only through collective measurements in general. When only *individual measurements* on single copies are available, we denote the minimum WMSE over locally unbiased measurements by

$$C(W) := \min_{(M, \hat{\theta}): \text{locally unbiased}} \text{Tr}(WV(M, \hat{\theta})) \quad (20)$$

$$= \min_M \text{Tr}(WI(M)^{-1}). \quad (21)$$

Note that $C(W)$ cannot be further improved even when separable, adaptive measurements across multiple copies of ρ_θ are available [30, 99]. While $C(W)$ is strictly larger than $C_H(W)$ in general, for pure states, $C(W) = C_H(W)$, and the HCRB is achievable through individual measurements [31].

2. Gill–Massar bound

Collective measurements (as experimentally demonstrated in [100]) can in general be much more powerful than individual measurements. It can be seen from the Gill–Massar (GM) bound [30] (see also Appx. D) that applies to all individual measurements. It states that for any d -dimensional quantum state ρ_θ and any (individual) POVM \tilde{M} ,

$$\text{Tr}(J^{-1}I(\tilde{M})) \leq d - 1. \quad (22)$$

It sets a lower bound on $\text{Tr}(JI(\tilde{M})^{-1})$ through Cauchy–Schwarz inequality,

$$\text{Tr}(JI(\tilde{M})^{-1}) \geq \frac{\text{Tr}(\mathbb{1})^2}{\text{Tr}(J^{-1}I(\tilde{M}))} \geq \frac{m^2}{d-1}. \quad (23)$$

For example, if we take $W = J$, $C_H(J) \leq 2m$ (easily seen from Eq. (19)), while $C(J) \geq m^2/(d-1)$ [30]. When the number of unknown parameters is $\Theta(d^2)$, e.g., in tomography, we have $C_H(J) = O(d^2)$ while $C(J) = \Omega(d^3)$ which is significantly larger than $C_H(J)$.

3. Fisher-symmetric measurements for pure states

Given a parameterized pure state ρ_θ , it was known that there exists a rank-one measurement M (with $2d-1$ measurement outcomes) such that the Fisher-symmetry condition is satisfied [47], i.e.,

$$I(M) = \frac{1}{2}J, \quad (24)$$

where $1/2$ is the best possible constant for state tomography, i.e., when the number of parameters $m = 2(d-1)$. One can see this from the GM bound—if $I(M) = cJ$ from some constant c , then $\text{Tr}(J^{-1}I(M)) = cm = 2c(d-1) \leq d-1$. (Note that although Eq. (24) was proven only for state tomography, it automatically holds for arbitrary m .)

The above measurement [47] is a function of the state ρ_θ and in practical implementation, must be adjusted adaptively based on the accumulated knowledge of the states [49]. In addition, both the computational complexity and implementation complexity of this approach can be costly. To overcome the limitation on

state-dependence, researchers studied universally Fisher-symmetric measurements that are independent of states. It was known the infinite-outcome Haar random measurements [101–104] are universally Fisher-symmetric and can achieve Eq. (24) for all pure states universally. However, they are experimentally infeasible because they require infinite amount of classical randomness and exponential gate complexity. In fact, [48] showed any measurement M satisfying Eq. (24) for all pure states must contain infinite number of measurement outcomes (and thus are not feasible). They proposed the 2-design collective measurements on two identical copies of the state as a workaround (as also experimentally demonstrated for the single-qubit case [100]). They showed that

$$I[\rho_\theta^{\otimes 2}, M] = J[\rho_\theta^{\otimes 2}], \quad (25)$$

when M is a 2-design measurement on 2 copies of any pure state ρ_θ . Here, we use $I[\star, M]$ ($J[\star]$) to denote the CFIM (QFIM) of the state \star , which is usually omitted in the expressions. In practice, implementing a two-copy measurement requires simultaneous access to and precise cross-device control of two identical quantum sensors. Consequently, a more experimentally accessible single-copy (individual) measurement protocol remains highly desirable. Our result partially resolves this challenge, providing feasible finite-outcome individual measurement protocols by tolerating a constant-factor suboptimality.

C. Definition of Near-Optimality

In this work, we will analyze the performance of randomized individual measurements for parameter estimation at a local point of θ . We define optimality conditions of measurements for families of quantum states where a constant-factor suboptimality is tolerated, in which case we use the term “near-optimal” to represent a potential constant-factor difference from the exact optimality. The near-optimality property is particularly important in situations where the optimal estimation precision can scale up or down with respect to system variables, e.g., the system dimension, the noise strength, the number of unknown parameters, etc. and near-optimality guarantees these scalings to be preserved across the entire range of system variables.

We first define quantum measurements that nearly saturate the QCRB by the following.

Definition 1 (Near-optimality). *A family of POVMs is near-optimal for a family of parameterized quantum states, if there exists a positive constant c (independent of the state or POVM) such that for any state in the family and its corresponding POVM M ,*

$$I(M) \succeq cJ. \quad (26)$$

Given a family of general mixed states, near-optimal individual measurements may not exist. For example, for maximally mixed states $\rho = \frac{1}{d}$ with maximal

number of unknown parameters, $C_F(J) = O(d^2)$ while $C(J) = \Omega(d^3)$, implying the $\Omega(d)$ gap between $I(M)$ and J . Therefore, we need a less stringent definition.

Definition 2 (Weak near-optimality). *A family of POVMs is weakly near-optimal for a family of parameterized quantum states, if there exists positive constants c_1, c_2 (independent of the state or POVM) such that for any state in the family and its corresponding POVM M ,*

$$\text{Tr}(J \cdot I(M)^{-1}) \leq c_1 \inf_{\tilde{M}: \text{POVM}} \text{Tr}(J \cdot I(\tilde{M})^{-1}), \quad (27)$$

$$I(M) \succeq c_2 \frac{\text{Tr}(J^{-1}I(M))}{m} J. \quad (28)$$

Recall m is the number of parameters. Eq. (27) implies the weak near-optimality measurement minimizes the WMSE up to a constant when the cost matrix is taken as the QFIM J . It guarantees the average near-optimal performance of M . Eq. (28) further guarantees the measurement provides an overall near-optimal estimation for all parameters, excluding the situation where the precision of some parameter is extremely low. We further explain and justify this definition in Appx. B. We prove whenever a near-optimal measurement exists, weak near-optimality is equivalent to near-optimality. We also explain how it functions as a proper generalization of the Fisher-symmetry condition [47–49].

Below we will see randomized measurements are (weakly) near-optimal in multiple interesting scenarios.

IV. PURE STATES

In this section, we consider randomized measurements for pure state metrology and obtain the following result.

Theorem 1. *When M is a POVM given by a 3-design, for any pure state ρ_θ and any number of parameters m ,*

$$I(M) \succeq \frac{d+2}{4(d+1)} J \succeq \frac{1}{4} J. \quad (29)$$

Here we use randomized measurements whose measurement basis forms a 3-design. Specifically, we say a randomized measurement is given by a 3-design if $M = \{M_s = q_s d |s\rangle\langle s|\}_s$, where $q_s > 0$ and $\sum_s q_s |s\rangle\langle s| = \mathbb{1}/d$. $\{|s\rangle, |s\rangle\}$ is called a (complex projective) 3-design [74, 75] if and only if

$$\sum_s q_s (|s\rangle\langle s|)^{\otimes 3} = \int_{\psi} (|\psi\rangle\langle\psi|)^{\otimes 3} d\psi, \quad (30)$$

where $d\psi$ is the (complex projective) Haar measure. One natural way to implement a 3-design measurement is to implement a random unitary U from a unitary 3-design [70, 76, 77] and then implement projection onto the computational basis. A unitary ensemble $\{q_i, U_i\}$ is a unitary 3-design if $\sum_i q_i U_i^{\otimes 3} \otimes U_i^{\dagger \otimes 3} = \int dU U^{\otimes 3} \otimes U^{\dagger \otimes 3}$

where dU is the Haar measure. For multi-qubit systems, random Clifford circuits form a unitary 3-design [78–80].

Theorem 1 implies for pure states, the QFIM is always saturable by 3-design randomized measurements up to a constant factor, i.e., they are near-optimal for pure states. This implies the *universal* optimality of 3-design randomized measurements for estimating any number of parameters in any pure states. Even in the context of single-parameter estimation, our method is still useful in providing an explicit measurement protocol that is always near-optimal for any parameterized pure states. In particular, the choice of randomized measurements do not rely on the knowledge of states or cost matrices (like in [31]), thus fit into the “measure first, ask questions later” framework [67] and substantially lower the complexity of experiments.

Before we prove Theorem 1. We first provide two useful properties [70, 105] of 3-designs that we will use later,

$$\sum_s q_s |s\rangle\langle s| \langle s|A|s\rangle = \frac{\text{Tr}(A)\mathbb{1} + A}{(d+1)d}, \quad (31)$$

$$\begin{aligned} & \sum_s q_s |s\rangle\langle s| \langle s|B|s\rangle \langle s|C|s\rangle = \\ & \frac{1}{(d+2)(d+1)d} \left((\text{Tr}(BC) + \text{Tr}(B)\text{Tr}(C))\mathbb{1} + \right. \\ & \left. \text{Tr}(B)C + \text{Tr}(C)B + \{B, C\} \right). \end{aligned} \quad (32)$$

Proof of Theorem 1. We prove Theorem 1 by explicitly constructing a set of locally unbiased estimators $\{\hat{\theta}_i\}_i$ that satisfy

$$V = \frac{4(d+1)}{d+2} J^{-1}, \quad (33)$$

where $V := V(M, \hat{\theta})$. This then implies Eq. (29) from the CRB (Eq. (2)) and the fact that $A \succeq B$ is equivalent to $A^{-1} \preceq B^{-1}$ for any positive matrices A, B . To construct locally unbiased estimators, we first introduce an unbiased estimator of ρ_θ using classical shadows [72],

$$\hat{\rho}(s) = \mathcal{M}^{-1}(|s\rangle\langle s|) = (d+1)|s\rangle\langle s| - \mathbb{1}, \quad (34)$$

where $\mathcal{M}(\cdot) = \frac{(\cdot) + \text{Tr}(\cdot)\mathbb{1}}{d+1}$, and \mathcal{M} is the inverse map of \mathcal{M} satisfying $\mathcal{M}^{-1}(\cdot) = (d+1)(\cdot) - \mathbb{1}$. $\hat{\rho}$ is an unbiased estimator of ρ_θ because

$$\mathbb{E}[|s\rangle\langle s|] := \sum_s \text{Tr}(\rho_\theta M_s) |s\rangle\langle s| = \mathcal{M}(\rho_\theta), \quad (35)$$

from Eq. (31), and then

$$\begin{aligned} \mathbb{E}[\hat{\rho}(s)] &= \mathbb{E}[\mathcal{M}^{-1}(|s\rangle\langle s|)] \\ &= \mathcal{M}^{-1}(\mathbb{E}[|s\rangle\langle s|]) = \rho_\theta. \end{aligned} \quad (36)$$

We then define the locally unbiased estimators at any local point $\theta = \theta^0$ by

$$\hat{\theta}_i(s; \theta^0) = \theta_i^0 + \text{Tr}((X_i|_{\theta=\theta^0})\hat{\rho}(s)), \quad (37)$$

where X_i are Hermitian operators which we will call *deviation observables* that satisfies the locally unbiasedness conditions

$$\text{Tr}(\rho_\theta X_i)|_{\theta=\theta^0} = 0, \text{Tr}((\partial_i \rho_\theta) X_j)|_{\theta=\theta^0} = \delta_{ij}, \forall i, j. \quad (38)$$

Here $\{X_i\}_{i=1}^m$ are named deviation observables because they are observables used to estimate the deviation of θ from θ^0 . X_i can vary for different θ but the dependence is omitted for simplicity. We will refer to estimators of form Eq. (37) as *local shadow estimators*, a type of locally unbiased estimator defined through deviation observables $\{X_i\}_i$.

To make sure Eq. (38) is satisfied, we choose

$$X_i = \sum_j (J^{-1})_{ij} L_j, \quad (39)$$

where L_j are SLDs. They satisfy $\text{Tr}(\rho_\theta L_j) = 0$ and $J_{ij} = \frac{1}{2} \text{Tr}(\rho_\theta \{L_i, L_j\})$ by definition. We can verify Eq. (8) and Eq. (9) at $\theta = \theta^0$ through

$$\begin{aligned} \mathbb{E}[\hat{\theta}_i(s; \theta^0)]|_{\theta=\theta^0} &= \theta_i^0 + \text{Tr}(X_i \rho_\theta)|_{\theta=\theta^0} = \theta_i^0, \quad (40) \\ (\partial_j \mathbb{E}[\hat{\theta}_i(s; \theta^0)]|_{\theta=\theta^0}) &= \text{Tr}(X_i|_{\theta=\theta^0} (\partial_j \rho_\theta)|_{\theta=\theta^0}) \\ &= \frac{1}{2} \sum_k (J^{-1})_{ik} \text{Tr}(\rho_\theta \{L_k, L_j\})|_{\theta=\theta^0} = \delta_{ij}. \quad (41) \end{aligned}$$

The MSEM obtained from this choice of deviation observables is at most a constant factor away from the inverse of the QFIM, as we desire. For any X_i and corresponding estimators (Eq. (37)), we have

$$\begin{aligned} V_{ij} &= \sum_s \text{Tr}(\rho_\theta M_s) (\hat{\theta}_i(s; \theta) - \theta_i) (\hat{\theta}_j(s; \theta) - \theta_j) \\ &= \sum_s q_s d \langle s | \rho_\theta | s \rangle \langle s | \mathcal{M}^{-1}(X_i) | s \rangle \langle s | \mathcal{M}^{-1}(X_j) | s \rangle \\ &= \frac{d+1}{d+2} \left(\text{Tr}(X_i X_j) + \text{Tr}(\rho_\theta \{X_i, X_j\}) \right) \\ &\quad - \frac{1}{d+2} \text{Tr}(X_i) \text{Tr}(X_j), \quad (42) \end{aligned}$$

where in the second equality we use the dual map of \mathcal{M}^{-1} is itself. The third equality is obtained by plugging in $\mathcal{M}^{-1}(X_i) = (d+1)X_i - \text{Tr}(X_i)\mathbb{1}$ and applying Eq. (32) and the first equality in Eq. (38).

Eq. (42) holds for any choice of X_i and any mixed ρ_θ . In the situation of pure states $\rho_\theta = |\psi\rangle\langle\psi|$ and definitions Eq. (39) of X_i , Eq. (42) can be further simplify by noticing that

$$L_i = 2(|\partial_i \psi\rangle\langle\psi| + |\psi\rangle\langle\partial_i \psi|), \quad (43)$$

$$\text{Tr}(L_i) = \text{Tr}(\rho_\theta L_i) = 0, \quad (44)$$

$$J_{ij} = 4\text{Re}[\langle\partial_i \psi|\partial_j \psi\rangle - \langle\psi|\partial_i \psi\rangle\langle\partial_j \psi|\psi\rangle], \quad (45)$$

$$\text{Tr}(L_i L_j) = 2J_{ij}. \quad (46)$$

Applying Eq. (42) and noticing the second term is zero, we have

$$(JVJ)_{ij} = \frac{d+1}{d+2} (\text{Tr}(L_i L_j) + \text{Tr}(\rho_\theta \{L_i, L_j\}))$$

$$= \frac{4(d+1)}{d+2} J_{ij}, \quad (47)$$

which implies Eq. (33) if we multiply both sides of the equation by J^{-1} on the left and right. \square

Traditionally, given any POVM $\{M_x\}_x$ (including the randomized measurement), it is always optimal to choose the locally unbiased estimator in Eq. (10) because it minimizes V and achieves $V = I(M)^{-1}$. However, a direct calculation of $I(M)$ is challenging because the randomization appears in both the denominator and the numerator of the expression. In contrast, our proof, which uses the local shadow estimator, only involves up to the third moment of the randomization (when calculating Eq. (42)), where 3-designs are sufficient. It is open whether 2-design measurements will be sufficient, and whether Theorem 1 can be further improved using other types of locally unbiased estimators and higher-order designs.

Note that in the proof of Theorem 1 (and in the proofs of other theorems below), we introduce the local shadow estimators (Eq. (37)), which are locally unbiased estimator that achieves the near-optimal estimation precision. For practical applications, one needs to first compute the deviation observables X_i through Eq. (39) and then performs randomized measurements on ρ_θ to estimate $\text{Tr}((X_i|_{\theta=\theta^0})\hat{\rho}(s))$ using $\hat{\rho}(s)$, the snapshots of classical shadow. Two caveats remain: (1) the deviation observable is a function of θ^0 which is not known a priori; (2) $\text{Tr}(X_i \hat{\rho}(s))$ may not be efficiently computable, both due to the difficulty in computing X_i and the difficulty in obtaining $\langle s | X_i | s \rangle$.

To tackle caveat (1), the two-step approach [28, 30, 41] is often adopted in quantum metrology, where a coarse estimate of θ is obtained first and X_i is then evaluated at the coarse estimate in order to calculate $\text{Tr}(X_i \hat{\rho}(s))$. Sec. VII contains an example of fidelity estimation where we numerically demonstrate the effectiveness of the two-step approach.

To address caveat (2), we need to leverage special structures of X_i and measurements. Below we consider a n -qubit system where the 3-design measurement is implemented through random Clifford sampling. Assume $|\psi_\theta\rangle$ and its derivatives $|\partial_i \psi_\theta\rangle$ are all restricted to a subspace spanned by a polynomial number of computational basis, which is a common scenario in quantum metrology. Then the total number of unknown parameters is at most a polynomial in n , which means X_i is efficiently computable because both the SLD L_i and the inverse of the QFIM J are efficiently computable. Furthermore, X_i can be decomposed into a polynomial number of computational basis operators, i.e., $X_i = \sum_{x,y \in \{0,1\}^n} f_{x,y} |x\rangle\langle y|$ where $f_{x,y} \neq 0$ only for polynomial numbers of x and y . Then $\text{Tr}(X_i \hat{\rho}(s))$ is efficiently computable because $|s\rangle$ is a stabilizer state and $\text{Tr}(|x\rangle\langle y| \hat{\rho}(s))$ is efficiently computable. In general, to efficiently compute X_i , we need both the SLD L_i and the inverse of the QFIM J to be

efficiently computable. The first condition is usually easily satisfiable for pure states that have efficient classical representations. The second condition is tractable in situations where J is diagonal or block-diagonal (see examples in Sec. VII A and Sec. VII C). To efficiently compute $\text{Tr}(X_i \hat{\rho}(s))$, further structures on X_i are needed, e.g., a stabilizer formalism that efficiently represents X_i (see an example in Sec. VII C), etc. We leave the study of general algorithms for computing X_i and sampling $\langle s|X_i|s \rangle$ for future work.

V. APPROXIMATELY LOW-RANK STATES

In this section, we consider a generalization of the previous result for pure states to *approximately low-rank well-conditioned states*. They include not only low-rank states, but also situations where the QFIM of some complex quantum states can be well approximated by confinement in a low-rank subspace. Previously, the optimality of low-rank states and their approximate (noisy) versions was not investigated in the context of either minimizing the WMSE or the local state tomography, to the best of our knowledge.

We define approximately low-rank well-conditioned states by the following.

Definition 3 (Approximately low-rank well-conditioned state). *A parameterized state ρ_θ is called an (μ, c) -approximately low-rank well-conditioned state if it satisfies the following two conditions:*

(1) *There is a constant μ such that there is at least one eigenvalue of ρ_θ that is at least μ .*

(2) *Let Π be the projector onto the subspace spanned by eigenstates of ρ_θ whose corresponding eigenvalues are at least μ . $\Pi_\perp = \mathbb{1} - \Pi$ and $p = \text{Tr}(\rho_\theta \Pi_\perp)$. There exists a constant c such that*

$$J - pJ^\perp - J^p \succeq cJ. \quad (48)$$

J^\perp is the QFIM after post-selecting on subspace Π_\perp , i.e., the QFIM of $\frac{\Pi_\perp \rho_\theta \Pi_\perp}{\text{Tr}(\rho_\theta \Pi_\perp)}$ and J^p is the CFIM of a Bernoulli distribution $\{p, 1-p\}$, i.e., $J_{ij}^p = \frac{(\partial_i p)(\partial_j p)}{p(1-p)}$.

Condition (1) above guarantees the existence of a low-rank approximation of the original state after projection to a low-rank subspace Π . Condition (2) guarantees the information of the unknown parameters are largely preserved after excluding the information from the subspace Π_\perp . This condition is necessary because we do not want the QFIM to concentrate on some high-dimensional subspace Π_\perp so that access to states in Π_\perp is required in which case any low-rank approximation will fail. Finally, it is worth noting that our definition implicitly assumes the states are well-conditioned within the subspace Π , i.e., the ratio between the largest and the smallest eigenvalues inside Π are bounded (because their eigenvalues

are above a constant μ). This is necessary because otherwise randomized measurements may not be near-optimal (see Sec. VII B). Pure states are a special case of approximately low-rank well-conditioned states with $\mu = 1$ and $c = 1$.

Below we first provide a proof of the near-optimality of randomized measurements when θ are encoded in a unitary rotation (which, in local parameter estimation, equivalently means the derivatives of all eigenvalues are zero). Then we provide generalization to all approximately low-rank well-conditioned states. The case of unitary rotations has a better constant and also serves as a perfect warm-up before introducing the general case.

Theorem 2. *Consider a (μ, c) -approximately low-rank well-conditioned state ρ_θ satisfying $\partial_j \lambda_j = 0$ for all of its eigenvalues λ_j . Let M be a POVM given by a 3-design. We have*

$$I(M) \succeq \frac{d+2}{d+1} \cdot \frac{\mu c}{2\mu+2} J. \quad (49)$$

Proof. We prove the theorem by finding locally unbiased estimators such that

$$V = V(M, \hat{\theta}) \preceq \frac{d+2}{d+1} \cdot \frac{2\mu+2}{\mu c} J^{-1}. \quad (50)$$

We adopt again local shadow estimators defined in Eq. (37) but will choose a different set of deviation observables X_i . They will satisfy $\Pi_\perp X_i \Pi_\perp = 0$ which plays a crucial role in bounding V , as we will see later. In the following, all functions are evaluated at some local point of θ implicitly. We define the unnormalized state $\rho_\perp := \Pi_\perp \rho_\theta \Pi_\perp$ for notation simplicity. We will also omit θ in ρ_θ .

Let L_i be the SLDs of ρ . We define

$$\begin{aligned} \tilde{L}_i &= L_i - \Pi_\perp L_i \Pi_\perp \\ &= 2 \sum_{j,k: \lambda_j \geq \mu \text{ or } \lambda_k \geq \mu} \frac{\langle \psi_j | \partial_i \rho | \psi_k \rangle}{\lambda_j + \lambda_k} |\psi_j\rangle \langle \psi_k|. \end{aligned} \quad (51)$$

Then

$$\begin{aligned} \text{Tr}(\rho \tilde{L}_i) &= 0 - \sum_{j: \lambda_j < \mu} \langle \psi_j | \partial_i \rho | \psi_j \rangle \\ &= 0 - \sum_{j: \lambda_j < \mu} \partial_i (\langle \psi_j | \rho | \psi_j \rangle) = -\partial_i p, \end{aligned} \quad (52)$$

$$\begin{aligned} \tilde{J}_{ij} &:= \text{Tr}(\tilde{L}_i \partial_j \rho) = \frac{1}{2} \text{Tr}(\rho \{\tilde{L}_i, L_j\}) \\ &= J_{ij} - \frac{1}{2} \text{Tr}(\rho_\perp \{\Pi_\perp L_i \Pi_\perp, \Pi_\perp L_j \Pi_\perp\}). \end{aligned} \quad (53)$$

where in the second line we use $\langle \partial_i \psi_j | \rho | \psi_j \rangle + \langle \psi_j | \rho | \partial_i \psi_j \rangle = \lambda_j (\partial_j \langle \psi_j | \psi_j \rangle) = 0$. Furthermore, we have $\partial_j \lambda_j = 0$, $\partial_i p = 0$ and $J^p = 0$. Moreover, the SLDs of the post-selected state $\frac{\rho_\perp}{\text{Tr}(\rho_\perp)}$ on subspace Π_\perp are $\Pi_\perp L_i \Pi_\perp$. They imply

$$\text{Tr}(\rho \tilde{L}_i) = 0, \quad \tilde{J} = \text{Tr}(\tilde{L}_i \partial_j \rho) = J - pJ^\perp. \quad (54)$$

Now we are ready to construct the locally unbiased estimators, defined through deviation observables

$$X_i = \sum_j (\tilde{J}^{-1})_{ij} \tilde{L}_j. \quad (55)$$

The locally unbiasedness condition is satisfied because

$$\text{Tr}(\rho X_i) = 0, \quad \tilde{J}_{ij} = \text{Tr}(X_i \partial_j \rho) = \delta_{ij}. \quad (56)$$

We can then evaluate V using Eq. (42). The second term is zero because $\text{Tr}(\tilde{L}_i) = \sum_{j:\lambda_j \geq \mu} \frac{\langle \psi_j | \partial_i \rho | \psi_j \rangle}{\lambda_j} = \sum_{j:\lambda_j \geq \mu} \partial_i \langle \psi_j | \psi_j \rangle = 0$. Therefore,

$$\tilde{J}V\tilde{J} = \frac{d+1}{d+2}(\tilde{K} + 2\tilde{J}), \quad (57)$$

where $\tilde{K}_{ij} := \text{Tr}(\tilde{L}_i \tilde{L}_j)$ and we use $\tilde{J}_{ij} = \frac{1}{2} \text{Tr}(\rho \{\tilde{L}_i, \tilde{L}_j\})$ which holds because $\text{Tr}(\rho \{\tilde{L}_i, \Pi_\perp L_j \Pi_\perp\}) = 0$. For any $\mathbf{v} \in \mathbb{R}^m$,

$$\begin{aligned} \mathbf{v}^T \tilde{K} \mathbf{v} &= 4 \sum_{jk:\lambda_j \geq \mu \text{ or } \lambda_k \geq \mu} \frac{|\langle \psi_j | \sum_i v_i \partial_i \rho | \psi_j \rangle|^2}{(\lambda_j + \lambda_k)^2} \\ &\leq \frac{4}{\mu} \sum_{jk:\lambda_j \geq \mu \text{ or } \lambda_k \geq \mu} \frac{|\langle \psi_j | \sum_i v_i \partial_i \rho | \psi_j \rangle|^2}{\lambda_j + \lambda_k} = \frac{2}{\mu} \mathbf{v}^T \tilde{J} \mathbf{v}. \end{aligned}$$

Therefore, $\tilde{K} \preceq \frac{2}{\mu} \tilde{J}$. Using Eq. (57), we have

$$V \preceq \frac{d+1}{d+2} \left(\frac{2}{\mu} + 2 \right) \tilde{J}^{-1}. \quad (58)$$

Condition (2) of the definition of approximately low-rank well-conditioned states guarantees $\tilde{J} \succeq cJ$, which then implies Eq. (50). \square

Theorem 2 is a generalization of **Theorem 1**—**Theorem 1** is directly implied from **Theorem 2** when taking $\mu = c = 1$ in **Theorem 2**. The key technique to prove **Theorem 2** is to choose the deviation observables wisely by excluding their components in subspace Π_\perp , which not only largely preserves the original QFIM but also makes upper bounding \tilde{K} via the QFIM possible.

Below, we consider the general case where unknown parameters can be encoded arbitrarily in the quantum state. We prove in this case, randomized measurements are still near-optimal for approximately low-rank well-conditioned states.

Theorem 3. Consider a (μ, c) -approximately low-rank well-conditioned state ρ_θ . Let M be a POVM given by a 3-design. We have

$$I(M) \succeq \frac{d+2}{d+1} \cdot \frac{\mu c^2}{2\mu c + 5} J. \quad (59)$$

Proof. We prove the theorem by finding locally unbiased estimators such that

$$V = V(M, \hat{\theta}) \preceq \frac{d+1}{d+2} \cdot \left(\frac{2}{c} + \frac{5}{\mu c^2} \right) J^{-1}. \quad (60)$$

Similar to the proof of **Theorem 2**, we adopt the local shadow estimators as our locally unbiased estimator, and use the unnormalized state $\rho_\perp := \Pi_\perp \rho \Pi_\perp$ for notation simplicity.

Let \tilde{L}_i be the SLDs of ρ . We define

$$\begin{aligned} \tilde{L}_i &= L_i - \Pi_\perp L_i \Pi_\perp + \frac{\partial_i p}{1-p} \Pi \\ &= \sum_{jk:\lambda_j \text{ or } \lambda_k \geq \mu} \left(\frac{2 \langle \psi_j | \partial_i \rho | \psi_k \rangle}{\lambda_j + \lambda_k} + \frac{\partial_i p}{1-p} \delta_{jk} \right) |\psi_j\rangle \langle \psi_k|. \end{aligned} \quad (61)$$

Then

$$\text{Tr}(\rho \tilde{L}_i) = 0 - \partial_i p + \partial_i p = 0, \quad (62)$$

$$\begin{aligned} \tilde{J}_{ij} &:= \text{Tr}(\tilde{L}_i \partial_j \rho) = \frac{1}{2} \text{Tr}(\rho \{\tilde{L}_i, L_j\}) \\ &= J_{ij} - p J_{ij}^\perp - J_{ij}^p. \end{aligned} \quad (63)$$

To verify Eq. (63) holds, we note that

$$\begin{aligned} J_{ii'}^\perp &= 2 \sum_{\substack{jk, \lambda_{j,k} < \mu, \\ \lambda_j + \lambda_k > 0}} \frac{\text{Re}[\langle \psi_j | \partial_i (\rho/p) | \psi_k \rangle \langle \psi_k | \partial_{i'} (\rho/p) | \psi_j \rangle]}{(\lambda_j + \lambda_k)/p} \\ &= \frac{2}{p} \sum_{\substack{jk, \lambda_{j,k} < \mu, \\ \lambda_j + \lambda_k > 0}} \frac{\text{Re}[\langle \psi_j | \partial_i \rho | \psi_k \rangle \langle \psi_k | \partial_{i'} \rho | \psi_j \rangle]}{\lambda_j + \lambda_k} - \frac{1-p}{p} J_{ii'}^p, \end{aligned}$$

where in the first equality we use the definition of QFIM and $\Pi_\perp \partial_i (\rho_\perp/p) \Pi_\perp = \Pi_\perp \partial_i (\rho/p) \Pi_\perp$. The second equality follows by direction calculations. Furthermore,

$$\tilde{J}_{ii'} = 2 \sum_{jk, \lambda_j \text{ or } \lambda_k \geq \mu} \frac{\text{Re}[\langle \psi_j | \partial_i \rho | \psi_k \rangle \langle \psi_k | \partial_{i'} \rho | \psi_j \rangle]}{\lambda_j + \lambda_k} - p J_{ii'}^p.$$

Combining the two equations above, we have $\tilde{J} + pJ^\perp + J^p = J$, which indicates Eq. (63).

Let the deviation observables be $X_i = \sum_j (\tilde{J}^{-1})_{ij} \tilde{L}_j$. The locally unbiasedness condition is satisfied because

$$\text{Tr}(\rho X_i) = 0, \quad \tilde{J}_{ij} = \text{Tr}(X_i \partial_j \rho) = \delta_{ij}. \quad (64)$$

Furthermore, let $\tilde{K}_{ij} = \text{Tr}(\tilde{L}_i \tilde{L}_j)$, we have, from Eq. (42),

$$\tilde{J}V\tilde{J} \preceq \frac{d+1}{d+2}(\tilde{K} + 2\tilde{J}). \quad (65)$$

Note that the second term in Eq. (42) is negative semidefinite and thus can be ignored because it can only decrease the right-hand side. As proved in **Appx. C**,

$$\tilde{K} \preceq \frac{5}{\mu} J. \quad (66)$$

Condition (2) of the definition of approximately low-rank well-conditioned states guarantees $\tilde{J} \succeq cJ$, which then implies

$$V \preceq \frac{d+1}{d+2} \left(\frac{5}{c\mu} \tilde{J}^{-1} + 2\tilde{J}^{-1} \right)$$

$$\asymp \frac{d+1}{d+2} \left(\frac{5}{\mu c^2} + \frac{2}{c} \right) J^{-1}. \quad (67)$$

□

Theorem 3 indicates that for any approximately low-rank well-conditioned state, which includes the cases where the eigenvalues of the quantum states depend on θ , randomized measurements can still be near-optimal.

VI. FULL-PARAMETER MIXED STATES

As discussed in [Sec. III C](#), near-optimal measurements do not exist for general mixed states. In these cases, it is meaningful to consider weak near-optimality ([Definition 2](#)). Here we provide several families of quantum states where near-optimal measurements generally do not exist, and 3-design randomized measurements are shown to be weakly near-optimal. The states discussed below are called *rank- r well-conditioned states*, which represent states which have r non-zero eigenvalues and the ratio between the largest and the smallest non-zero eigenvalues are upper bounded by a constant.

Theorem 4. *When M is a POVM given by a 3-design, it is weakly near-optimal for the following family of states:*

- (1) *Rank- r well-conditioned states, whose number of unknown parameters is maximal, i.e., $m = r(2d - r) - 1$.*
- (2) *Rank- r well-conditioned states ρ_θ that satisfies $\Pi \partial_i \rho_\theta \Pi = \partial_i \rho_\theta$ for all i where Π is the projection onto the support of ρ_θ , whose number of unknown parameters is maximal, i.e., $m = r^2 - 1$.*
- (3) *Rank- r well-conditioned states ρ_θ that satisfies $\Pi \partial_i \rho_\theta \Pi = 0$ for all i where Π is the projection onto the support of ρ_θ , whose number of unknown parameters is maximal, i.e., $m = 2r(d - r)$.*

Case (1) is the standard case of estimating a full-parameter rank- r quantum state. Case (2) describes the situation where randomized measurements act on a larger Hilbert space than the Hilbert space ρ_θ lives in, which is common in situations where ρ_θ is restricted to a small subspace of the actual physical system. Case (3) describes the situation where the unknown parameters are encoded in the derivatives of ρ_θ which takes ρ_θ outside its support, with a typical example being pure states. A non-trivial example would be $\rho_\theta = U_\theta \rho_0 U_\theta^\dagger$ where θ is encoded in some unitary rotation U_θ and ρ_0 is the rank- r maximally mixed state Π/r independent of θ . Note that here the rank r can scale non-trivially with respect to the system dimension d and the weak near-optimality in the three cases above does not imply one another.

Proof of Theorem 4. Here we consider rank- r well-conditioned states. In particular, we assume the condition number inside the support of the state

$$\kappa = \frac{\max_i \lambda_i}{\min_{i: \lambda_i > 0} \lambda_i} \quad (68)$$

is a constant. Note that $\min_{i: \lambda_i > 0} \lambda_i \geq 1/(r\kappa)$.

To show weak near-optimality, we will find locally unbiased estimators such that $\text{Tr}(JV)$, where V is the MSEM with respect to it, is at most a constant factor away from its minimum value. Again, we adopt local shadow estimators ([Eq. \(37\)](#)) for the proof and use [Eq. \(42\)](#) to evaluate $\text{Tr}(JV)$. The deviation observables $\{X_i\}_i$ are defined by

$$X_i = \sum_j (J^{-1})_{ij} L_j, \quad (69)$$

where L_i are the SLDs. Let

$$K_{ij} := \text{Tr}(L_i L_j) = 4 \sum_{k\ell: \lambda_k + \lambda_\ell > 0} \frac{\text{Re}[\langle \psi_k | \partial_i \rho_\theta | \psi_\ell \rangle \langle \psi_\ell | \partial_j \rho_\theta | \psi_k \rangle]}{(\lambda_k + \lambda_\ell)^2}. \quad (70)$$

For any $\mathbf{v} \in \mathbb{R}^m$,

$$\begin{aligned} \mathbf{v}^T K \mathbf{v} &= 4 \sum_{k\ell: \lambda_k + \lambda_\ell > 0} \frac{|\langle \psi_k | \sum_i v_i \partial_i \rho_\theta | \psi_\ell \rangle|^2}{(\lambda_k + \lambda_\ell)^2} \\ &\leq 4r\kappa \sum_{k\ell: \lambda_k + \lambda_\ell > 0} \frac{|\langle \psi_k | \sum_i v_i \partial_i \rho_\theta | \psi_\ell \rangle|^2}{\lambda_k + \lambda_\ell} = 2r\kappa \mathbf{v}^T J \mathbf{v}, \end{aligned}$$

which implies $K \preceq 2r\kappa J$. From [Eq. \(42\)](#) and the CR bound $I(M)^{-1} \preceq V$, we have

$$JVJ \preceq \frac{(d+1)}{d+2} (2J + K) \preceq \frac{2(d+1)(1+r\kappa)}{d+2} J, \quad (71)$$

which implies

$$\text{Tr}(JI(M)^{-1}) \leq \text{Tr}(JV) \leq \frac{2(d+1)(1+r\kappa)m}{d+2}, \quad (72)$$

and, if we multiply both sides by $J^{-1/2}$ on the left and right and take the inverse,

$$I(M) \succeq \frac{d+2}{2(d+1)(1+r\kappa)} J. \quad (73)$$

Below we use the GM bound ([Eq. \(22\)](#) [[30](#)], see also [Appx. D](#)), to put upper bounds on $\text{Tr}(J^{-1}I(M))$ put lower bounds on $\text{Tr}(JI(\tilde{M})^{-1})$ for general \tilde{M} that match the scalings of the upper bounds in [Eq. \(72\)](#) in different cases.

When ρ_θ belongs to case (1), i.e., is a rank- r well-conditioned state with maximal number of parameters. We have

$$m = r^2 - 1 + 2(d-r)r = r(2d-r) - 1 = \Theta(rd), \quad (74)$$

where $r^2 - 1$ corresponds to the degrees of freedom within the support of ρ_θ and $2(d-r)r$ corresponds to the degrees of freedom outside the support of ρ_θ . In this case, the upper bound ([Eq. \(72\)](#)) and the lower bound ([Eq. \(23\)](#)) on $\text{Tr}(JI(M)^{-1})$ are both $\Theta(r^2d)$. Also note

that $\text{Tr}(J^{-1}I(M)) \leq d - 1$ by GM bound. These indicate the weak near-optimality of the randomized measurement M .

In case (2), both ρ_θ and its derivatives $\partial_i \rho_\theta$ are restricted to the r -dimensional support of ρ_θ . $m = r^2 - 1$. As shown in Appx. D, the GM bound can be tightened into

$$\text{Tr}(J^{-1}I(\tilde{M})) \leq r - 1, \Rightarrow \text{Tr}(JI(\tilde{M})^{-1}) \geq \frac{m^2}{r - 1}. \quad (75)$$

In this case, the upper bound (Eq. (72)) and the lower bound (Eq. (75)) on $\text{Tr}(JI(M)^{-1})$ are both $\Theta(r^3)$, indicating the weak near-optimality of the randomized measurement M .

In case (3), the derivatives $\partial_i \rho_\theta$ are restricted to the off-diagonal block orthogonal to the support of ρ_θ . $m = 2r(d - r)$. As shown in Appx. D, the GM bound can be tightened into

$$\text{Tr}(J^{-1}I(\tilde{M})) \leq d - r, \Rightarrow \text{Tr}(JI(\tilde{M})^{-1}) \geq \frac{m^2}{d - r}. \quad (76)$$

In this case, the upper bound (Eq. (72)) and the lower bound (Eq. (76)) on $\text{Tr}(JI(M)^{-1})$ are both $\Theta(r^2(d - r))$, indicating the weak near-optimality of the randomized measurement M . \square

Theorem 4 demonstrates three cases of mixed states where randomized measurements are weakly near-optimal. The requirement that the states must have the maximal number of unknown parameters can be slightly relaxed—the theorem still holds as long as the scaling of the actual m is the same as the scaling of the maximal number.

We remark that in the special case of full-parameter maximally mixed states ($r = d$, $\kappa = 1$), a direct computation of the CFIM [48] showed 2-design measurements are sufficient to achieve $I(M) = \frac{J}{d+1}$ and thus weakly near-optimal. 3-designs are unnecessary in this case. In general, however, it is unclear whether 2-design measurements will be sufficient for estimating full-parameter rank- r states.

VII. EXAMPLES

In this section, we provide three examples to demonstrate the power and limitation of randomized measurements in multi-parameter quantum metrology. We also explicitly compute the deviation observables in several cases, and illustrate the advantage of local shadow estimators in one numerical example of fidelity estimation.

A. Fidelity Estimation: Pure States

1. Theory

Here we consider estimating the fidelity of a parameterized pure state to a fixed quantum state. According to

Theorem 1, randomized measurements are near-optimal in this case. Without loss of generality, we assume

$$|\psi_\theta\rangle := |\psi_{f,g}\rangle = \sqrt{f}|\phi\rangle + \sqrt{1-f}|\phi_g^\perp\rangle, \quad (77)$$

where $f := |\langle\phi|\psi_\theta\rangle|^2$ is the fidelity of $|\psi_\theta\rangle$ to a fixed state $|\phi\rangle$, and $|\phi_g^\perp\rangle$ is orthogonal to $|\phi\rangle$. Specifically, we let $\theta_1 = f$ and $(\theta_2, \theta_3, \dots, \theta_m) = g$. $|\phi_g^\perp\rangle$ depends on g but $|\phi\rangle$ is independent of it. Here we explicitly calculate the MSE of estimating f using the randomized measurement and the local shadow estimator defined in the proof of **Theorem 1**, which can be shown to be optimal. First, note that

$$J_{ff} = 4\text{Re}[\langle\partial_f\psi|\partial_f\psi\rangle - \langle\psi|\partial_f\psi\rangle\langle\partial_f\psi|\psi\rangle] = \frac{1}{f(1-f)}. \quad (78)$$

and, for any i ,

$$J_{fg_i} = 4\text{Re}[\langle\partial_f\psi|\partial_{g_i}\psi\rangle - \langle\psi|\partial_f\psi\rangle\langle\partial_{g_i}\psi|\psi\rangle] = 0. \quad (79)$$

The QFIM is block-diagonal. From Eq. (39), the deviation observable should be taken as $X_f = \frac{L_f}{J_{ff}}$, i.e.,

$$X_f = 2f(1-f)|\phi\rangle\langle\phi| - 2f(1-f)|\phi_g^\perp\rangle\langle\phi_g^\perp| + (1-2f)\sqrt{f(1-f)}(|\phi\rangle\langle\phi_g^\perp| + |\phi_g^\perp\rangle\langle\phi|), \quad (80)$$

and, from Eq. (42), the MSE for estimating f is

$$\begin{aligned} V_{ff} &= \frac{d+1}{d+2}(\text{Tr}(X_f^2) + 2\langle\psi|X_f^2|\psi\rangle) \\ &= \frac{4(d+1)}{d+2}f(1-f). \end{aligned} \quad (81)$$

Now we explicitly compare the performance of the randomized measurement and local shadow estimator with two other standard and widely used estimators.

(1) **Optimal measurement and estimator.** The projective measurement $M^{\text{opt}} = \{|\phi\rangle\langle\phi|, \mathbb{1} - |\phi\rangle\langle\phi|\}$ is optimal for fidelity estimation. The probability distribution of the projective measurement is $\{f, 1-f\}$ and then we have

$$I(M^{\text{opt}})_{ff} = \frac{1}{f(1-f)}, \quad I(M^{\text{opt}})_{fg_i} = 0, \quad \forall i. \quad (82)$$

Then the minimum MSE $V_{ff} = (I(M^{\text{opt}})^{-1})_{ff} = f(1-f) = (J^{-1})_{ff}$ is achieved by the corresponding optimal locally unbiased estimator (see Eq. (10)). We see above that randomized measurements can achieve the same MSE up to a constant factor $4(d+1)/(d+2)$, as also proved in **Theorem 1**. In practice, randomized measurements can be more advantageous than the optimal binary measurement in situations where the latter is challenging to implement, e.g., when $|\phi\rangle$ is highly entangled. Also, the choice of randomized measurements do not depend on $|\phi\rangle$ while the projective measurement must.

(2) Standard shadow estimator. Another standard method [72] to estimate fidelity using randomized measurements is to use the standard shadow estimator which is also a locally unbiased estimator defined by

$$\hat{f}^{\text{std}}(s) = \langle \phi | \hat{\rho}(s) | \phi \rangle, \quad (83)$$

where $\hat{\rho}(s)$ is defined in Eq. (34). When the measurement is given by a 3-design, the corresponding MSE is

$$V_{ff}^{\text{std}} = \frac{2(d+1)(1+2f)}{d+2} - (1+f)^2. \quad (84)$$

In contrast to the local shadow estimator which is only unbiased in the vicinity of its true value, the standard shadow estimator is globally unbiased and independent of the state and the parameters. However, the MSE obtained is not as small as the MSE obtained using the local shadow estimator. We have, for any f and d , $V_{ff}^{\text{std}} \geq V_{ff}$, and the equality holds only when $f = 1/2$ and $d = 2$.

In particular, when the fidelity f approaches 1, which means the quantum state $|\psi_\theta\rangle$ is close to the target state $|\phi\rangle$, we have $V_{ff} \rightarrow 0$, while $V_{ff}^{\text{std}} \rightarrow \frac{2(d-1)}{d+2}$ remains a positive constant. It indicates a fundamental advantage of local shadow estimators over standard shadow estimators.

2. Numerical simulation

To demonstrate the practical feasibility and advantages of our methods, we numerically implement a pipeline of pure state fidelity estimation using the local shadow estimator, and compare it with the standard shadow estimator [72] (Eq. (83)). Our simulation is conducted using Qiskit [108]. The data and codes are available online (see the Data Availability section).

Our theoretical framework assumes knowing a fiducial state that is sufficiently close to the true unknown state, so that we can define the local shadow estimator (and deviation observable) with respect to that fiducial state. To apply this theory in practice, we adopt the following post-processing algorithm (after N copies of states are measured using individual 3-design measurements). One first obtains a coarse estimate of (f^0, g^0) describing the unknown state (in the form of Eq. (77)) using, e.g., standard classical shadow [72], and set it as the initial fiducial state. One can then use the initial fiducial state to compute the deviation observable (Eq. (80)) and evaluate the local shadow estimator through

$$f^1 = f^0 + \frac{1}{N} \sum_s \text{Tr}(X_{f^0} \hat{\rho}(s)), \quad (85)$$

and update the estimator \hat{f} from f^0 to f^1 . Note that updating \hat{g} is unnecessary because their influence on \hat{f} is only second-order from the locally unbiasedness condition and can be ignored when the initial guess (f^0, g^0) is

sufficiently close to their true values. The above updating procedure is repeated and terminates at step k when the stepwise change $|f^k - f^{k-1}|$ converges below a small cutoff number, e.g., 10^{-6} . Remarkably, the entire algorithm operates by reusing the same set of measurement data, which means there is no sampling overhead of our methods compared to standard shadow estimator. Our protocol is summarized in Algorithm 1.

Algorithm 1: Local Shadow Fidelity Estimation

Input : Target state $|\phi\rangle$ and unknown state $|\psi\rangle$
Output: Estimate of fidelity $f = |\langle \phi | \psi \rangle|^2$
1 Repeat N randomized measurements on $|\psi\rangle$'s
2 Obtain N snapshots of classical shadow $\{\hat{\rho}(s)\}_s$
3 Coarsely estimate \hat{f} and \hat{g} from snapshots $\{\hat{\rho}(s)\}_s$
4 **repeat**
5 Compute $X_{\hat{f}}$ using \hat{f}, \hat{g} via Eq. (80)
6 $\hat{\Delta} \leftarrow \frac{1}{N} \sum_s \text{Tr}(X_{\hat{f}} \hat{\rho}(s))$
7 $\hat{f} \leftarrow \hat{f} + \hat{\Delta}$
8 **until** $\hat{\Delta} <$ some cutoff value
9 **return** \hat{f}

As a concrete example, let us consider the following parameterized family of n -qubit pure states,

$$|\psi_\varphi\rangle = \sqrt{\varphi_0} |\Phi\rangle + \sum_{i=1}^n \sqrt{\varphi_i} |\Phi_i\rangle, \quad (86)$$

where $\varphi_0 = 1 - \sum_{i=1}^n \varphi_i$, $|\Phi\rangle = \frac{1}{\sqrt{2}}(|0\rangle^{\otimes n} + |1\rangle^{\otimes n})$ is the n -qubit GHZ state and $|\Phi_i\rangle = (\sigma_x)_i |\Phi\rangle$ is the GHZ with bit-flip on the i -th qubit. We choose $n = 3$ and choose the target state $|\phi\rangle$ from fidelity estimation to be the one with parameters $\varphi_1 = \varphi_2 = \varphi_3 = 0.075$. (Note this target state is not a stabilizer state and its projector cannot be implemented via Clifford gates.) We estimate the fidelity of four unknown states to $|\phi\rangle$ where $\varphi_1 = \varphi_2 = \varphi_3 = 0.10, 0.15, 0.20, 0.25$, yielding the true infidelities $1 - f = 0.0073, 0.0570, 0.1459, 0.2759$, respectively.

We implement Algorithm 1 to estimate fidelity from $N = 5000$ randomized measurements and compare it to the standard shadow estimator (Eq. (83)). Specifically, we obtain the initial coarse estimates $\{\hat{\varphi}_i\}_{i=1}^3$ by computing the overlap between $|\psi_\varphi\rangle$ and $|\Phi_i\rangle$ using the standard shadow estimator

$$\hat{\varphi}_i = \frac{1}{N} \sum_s \langle \Phi_i | \hat{\rho}(s) | \Phi_i \rangle. \quad (87)$$

We then compute the initial $\hat{f} = f^0 = |\langle \phi | \psi_{\hat{\varphi}} \rangle|^2$ and start to repetitively compute the local shadow estimators and update \hat{f} until the stepwise difference is below 10^{-6} . We compare the performance of Algorithm 1 to the standard shadow estimator $\hat{f}^{\text{std}} = \frac{1}{N} \sum_s \langle \phi | \hat{\rho}(s) | \phi \rangle$. Both methods use exactly the same amount of experimental data and the difference is Algorithm 1 adopts an additional post-processing procedure.

Our simulation results are reported in Fig. 3. To demonstrate and compare the performances of both esti-

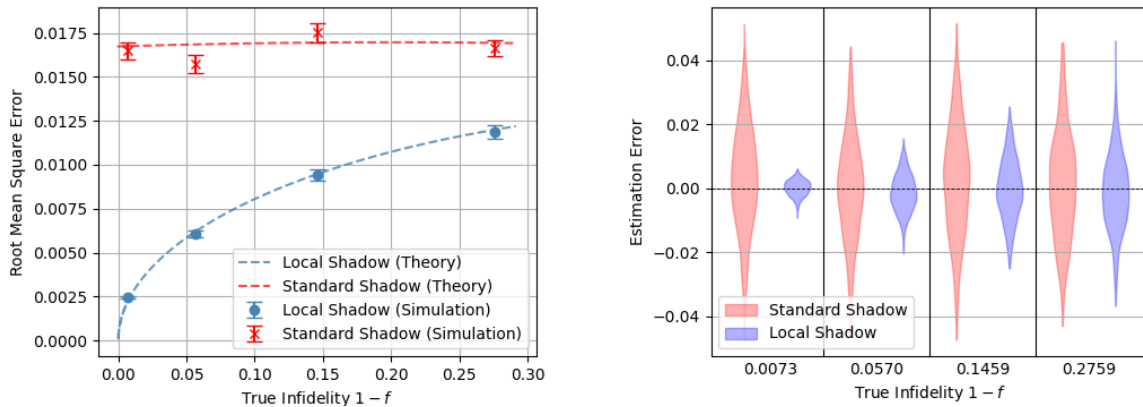


Figure 3. Simulation of a 3-qubit pure state fidelity estimation task comparing standard and local shadow estimators. The target state $|\phi\rangle$ and four unknown states with different infidelities all come from a 3-parameter family of pure states described in Sec. VII A 2. For each unknown state, we build a dataset by uniformly sampling 100,000 random Clifford and measuring each for 10,000 shots. We then subsample 500 batches from the dataset, each consists of $N = 5000$ random Clifford and a single shot of measurement. (Left.) Comparison of theoretical (square roots of Eq. (81) and Eq. (84), divided by \sqrt{N}) and empirical (averaged over 500 batches of subsamples) root mean squared error (RMSE) of estimators. Error bars depict one standard error estimated via 200 round of bootstrap sampling [106]. (Right.) Violin plots (smoothed histograms [107]) of estimation errors from 500 batches of subsamples for the four unknown states labeled by the corresponding infidelity. The variance of our local shadow estimator decreases as the true infidelity decreases, whereas the variance of the standard shadow estimator remains nearly constant.

estimators, we create a large dataset containing many random Clifford and measurement shots, and then subsampling 500 batches of data to construct estimators and estimate their variance. Note that subsampling is a well-established method to assess the estimator variance while avoid the computational burden of full re-sampling [106]. See the caption of Fig. 3 for more details. We also plot our theoretic predictions of the root mean squared error (RMSE, i.e., square root of the MSE) given by $\frac{1}{\sqrt{N}} \times$ the square roots of the single-shot MSE in Eq. (81) and Eq. (84). The factor of $\frac{1}{\sqrt{N}}$ arises because the snapshots $\hat{\rho}(s)$ are i.i.d. For all values of fidelity simulated, the theoretical predictions agree with the empirical RMSEs within the error bars. Notably, though the MSE formula in Eq. (81) was derived in the context of local estimation, it also accurately captures the MSE for our Algorithm 1 where no prior knowledge of f is provided. The advantage of local shadow estimators over standard shadow estimators, as predicted by Eq. (81) and Eq. (84) is then established numerically.

Regarding the run time of Algorithm 1, we observe that in most cases no more than 5 repetitions are sufficient for the stepwise change of \hat{f} to converge below 10^{-6} .

B. Fidelity Estimation: Mixed States

In contrast to the previous section, here we will show a no-go example where randomized measurements cannot be near-optimal—fidelity estimation for mixed states. Specifically, consider the following single-parameter fam-

ily of d -dimensional quantum states

$$\rho_f := f|\phi\rangle\langle\phi| + (1-f) \frac{\mathbb{1} - |\phi\rangle\langle\phi|}{d-1}, \quad (88)$$

for some fixed pure state $|\phi\rangle$. ρ_f can be understood as $|\phi\rangle$ going through a depolarizing channel, and our goal is to estimate the fidelity $f := \langle\phi|\rho|\phi\rangle$. Below we consider the regime where $1-f \leq d^{-2}$, which means the mixed state ρ_f is very close to the target state $|\phi\rangle$. The QFI for ρ_f is easily seen to be

$$J_{ff} = \frac{1}{f(1-f)}, \quad (89)$$

We now show that randomized measurements are not near-optimal for this task. In particular, this holds for any d (even when $d = 2$). Since weak near-optimality is equivalent to near-optimality in single-parameter metrology tasks, randomized measurements are also not weakly near-optimal here.

Let us first clarify our definition of randomized measurements here. The results we present in Sec. IV–Sec. VI are sufficient conditions for randomized measurements to be near-optimal or weakly near-optimal. For all these results, it suffices to take the POVM as any 3-design. To derive no-go results, however, we need to specify the exact choice of the POVMs. Below we prove the no-go results when the POVM exactly forms a (complex projective) Haar measure, and when it is a specific 3-design.

(1) Haar measure. Let the POVM element be $M^{\text{Haar}} = \{d d\mu_s|s\rangle\langle s|\}_s$, where $\{d\mu_s|s\rangle\langle s|\}_s$ is the (complex projective) Haar measure for d -dimensional pure states [68].

Note that the dimension d should be distinguished from the differential symbol d . The probability density $p_s := \text{Tr}(\frac{dM_s^{\text{Haar}}}{d\mu_s}\rho_f)$ is

$$p_s = d \left(f |\langle s|\phi\rangle|^2 + (1-f) \frac{1 - |\langle s|\phi\rangle|^2}{d-1} \right). \quad (90)$$

Define $\tau_s := |\langle s|\phi\rangle|^2$. The CFI can be calculated to be

$$\begin{aligned} I(M^{\text{Haar}})_{ff} &= \int d\mu_s \frac{(\partial_f p_s)^2}{p_s} \\ &= \frac{d}{(d-1)^2} \int d\mu_s \frac{(1-\tau_s d)^2}{f\tau_s + (1-f)\frac{1-\tau_s}{d-1}}. \end{aligned} \quad (91)$$

Dividing the integral over s into two parts depending on whether $\tau_s < \sqrt{1-f}$ holds or not, we have the following upper bound,

$$\begin{aligned} I(M^{\text{Haar}})_{ff} &\leq \frac{d}{(d-1)^2} \left(\int_{\tau_s > \sqrt{1-f}} d\mu_s \frac{(1-\tau_s d)^2}{\sqrt{1-f}} \right. \\ &\quad \left. + \int_{\tau_s \leq \sqrt{1-f}} d\mu_s \frac{(1-\tau_s d)^2}{(1-f)\frac{1}{d-1}} \right) \\ &\leq \frac{d}{d-1} \left(\frac{d-1}{\sqrt{1-f}} + \frac{\text{Pr}[\tau_s \leq \sqrt{1-f}]}{1-f} \right). \end{aligned} \quad (92)$$

In the first inequality, we use $f\tau_s + (1-f)\frac{1-\tau_s}{d-1} \geq (1-f)\frac{1}{d-1}$ and, when $\tau_s \geq \sqrt{1-f}$ and $\sqrt{1-f} \leq d^{-1}$, $f\tau_s + (1-f)\frac{1-\tau_s}{d-1} \geq \sqrt{1-f}$. In the second inequality, we use the fact that $(1-\tau_s d)^2 \leq (d-1)^2$ and that, when $\tau_s \leq \sqrt{1-f} \leq d^{-1}$, $(1-\tau_s d)^2 \leq 1$. In [Appx. E](#), we show that $\text{Pr}[\tau_s \leq \sqrt{1-f}] \leq (d-1)\sqrt{1-f}$. Thus, we have

$$I(M^{\text{Haar}})_{ff} \leq \frac{2d}{\sqrt{1-f}}, \quad (93)$$

$$\Rightarrow \frac{I(M^{\text{Haar}})_{ff}}{J_{ff}} \leq 2d\sqrt{1-f}f. \quad (94)$$

When taking $1-f \rightarrow 0$, we have $\frac{I(M^{\text{Haar}})_{ff}}{J_{ff}} \rightarrow 0$. This completes the proof that M^{Haar} is not near-optimal.

(2) 3-design. For completeness, we now give another example that a specific POVM forming a 3-design is not near-optimal for mixed state fidelity estimation. Take [Eq. \(88\)](#) to be an single-qubit state.

$$\rho_f = f|\phi\rangle\langle\phi| + (1-f)|\phi^\perp\rangle\langle\phi^\perp|. \quad (95)$$

where $|\phi^\perp\rangle\langle\phi^\perp| := \mathbb{1} - |\phi\rangle\langle\phi|$. Consider single-qubit random Pauli measurements

$$M^P = \left\{ \frac{1}{3}|x\pm\rangle\langle x\pm|, \frac{1}{3}|y\pm\rangle\langle y\pm|, \frac{1}{3}|z\pm\rangle\langle z\pm| \right\}. \quad (96)$$

Here $|x\pm\rangle$ denotes the ± 1 eigenstate for Pauli X, similar for the others. M^P forms a (complex projective) 3-design satisfying [Eq. \(30\)](#). Now choose

$$|\phi\rangle\langle\phi| := \frac{1}{2} \left(\mathbb{1} + \frac{1}{\sqrt{3}}(\sigma_x + \sigma_y + \sigma_z) \right). \quad (97)$$

In the Bloch sphere, $|\phi\rangle$ is located equidistant from $|x+\rangle$, $|y+\rangle$, and $|z+\rangle$. With some calculation, one can obtain the measurement outcome probability and the CFI as

$$\begin{aligned} p_{a\pm} &:= \text{Tr}(\rho_f M_{a\pm}^P) = \frac{1}{6} \left(1 \pm \frac{2f-1}{\sqrt{3}} \right), \quad \forall a \in \{x, y, z\}, \\ I(M^P)_{ff} &= \frac{2}{1+2f(1-f)}, \end{aligned} \quad (98)$$

When we take $1-f \rightarrow 0$, we have $\frac{I(M^P)_{ff}}{J_{ff}} \rightarrow 0$, thus M^P is not near-optimal despite being a 3-design. As a final comment, if we rotate M^P such that $|\phi\rangle\langle\phi|$ is proportional to one of the POVM elements, then the measurement yields a CFI of $\frac{1}{3}J_{ff}$ and is thus near-optimal. However, such choices of measurement are tailored to the state, and thus should not be viewed as a generic randomized measurement for our purpose.

C. Hamiltonian Estimation

Finally, we provide one example of quantum *channel estimation*, which goes beyond the previously discussed *state estimation* problem.

We will see that [Theorem 1](#) and [Theorem 2](#) can be applied in a Hamiltonian estimation problem in the noiseless and the noisy case, respectively. Specifically, we consider the estimation of all Pauli operators in a Hamiltonian and show two near-optimal estimation protocols minimizing the WMSE with $W = \mathbb{1}$, one utilizing maximally entangled states and the other one utilizing random stabilizer states as input states. 3-design randomized measurements are near-optimal in both the noiseless case (from [Theorem 1](#)) and the noisy case (from [Theorem 2](#)).

1. Noiseless case

We consider a Hamiltonian estimation problem in an n -qubit system, where

$$U_\theta = \exp \left(-i \sum_{k=1}^{d^2-1} \theta_k P_k \right), \quad (99)$$

where $d = 2^n$ and $\{P_k\}_{k=1}^{d^2-1}$ are the set of multi-qubit Pauli operators $\{\mathbb{1}, \sigma_x, \sigma_y, \sigma_z\}^{\otimes n}$ excluding $\mathbb{1}$. Consider parameter estimation at $\theta = 0$ for pure input states¹. Let the input state of the unitary evolution be $|\psi\rangle$, we have the QFIM $J(\psi)$ of the output state

$$|\psi_\theta\rangle := U_\theta |\psi\rangle \quad (100)$$

¹ All functions we calculate in this section will be implicitly evaluated at $\theta = 0$, unless specified otherwise.

equal to

$$\begin{aligned} J(\psi)_{jk} &= 4\text{Re}[\langle \partial_j \psi_\theta | \partial_k \psi_\theta \rangle - \langle \psi_\theta | \partial_j \psi_\theta \rangle \langle \partial_k \psi_\theta | \psi_\theta \rangle] \\ &= 4\langle \psi | \frac{1}{2} \{P_j, P_k\} | \psi \rangle - \langle \psi | P_j | \psi \rangle \langle \psi | P_k | \psi \rangle, \end{aligned} \quad (101)$$

where we use $J(\star)^2$ to denote the QFIM when the input state is \star .

• Figure of merit

Different choices of input states $|\psi\rangle$ lead to different performances of Hamiltonian estimation. To evaluate their performances, we will use the trace of the inverse of the CFIM as a function of the input state ψ and the measurement M , i.e.,

$$\text{Tr}(I(\psi, M)^{-1}) \quad (102)$$

as the figure of merit. The function $\text{Tr}(I(\psi, M)^{-1})$ can be interpreted as the minimum achievable WMSE (according to the CRB) with the cost matrix $W = \mathbb{1}^3$, when the input state is $|\psi\rangle$ and the measurement is M . The above can be generalized to the case where we use an input state ensemble to estimate the Hamiltonian, instead of a single input state. Specifically, we can assume, with probability $p^{(i)}$, we pick $|\psi^{(i)}\rangle$ as an input state and $M^{(i)}$ as the corresponding POVM. Then we use $I(\{p^{(i)}, \psi^{(i)}, M^{(i)}\})$ to denote the corresponding CFIM. In particular, we have

$$I(\{p^{(i)}, \psi^{(i)}, M^{(i)}\}) \quad (103)$$

$$= I\left(\sum_i p_i |i\rangle \langle i|_{\text{R}} \otimes \psi^{(i)}, \sum_i p_i |i\rangle \langle i|_{\text{R}} \otimes M^{(i)}\right) \quad (104)$$

$$= \sum_i p^{(i)} I(\psi^{(i)}, M^{(i)}), \quad (105)$$

where we introduce the fictitious reference system R to facilitate the calculation.

Below, we consider two types of input state ensembles for the Hamiltonian estimation problem. We will see they are both near-optimal and are equivalent up to a constant factor. Here, we say an input state ensemble (along with a corresponding measurement) is *near-optimal*, if it achieves the minimum WMSE optimized over all input state ensembles and measurements, i.e.,

$$w := \inf_{\{p^{(i)}, \psi^{(i)}, M^{(i)}\}} \text{Tr}(I(\{p^{(i)}, \psi^{(i)}, M^{(i)}\})^{-1}) \quad (106)$$

² This notation should be distinguished from $J[\star]$ which is the QFIM of the parameterized state \star that we use later.

³ Here it is not suitable to choose the cost matrix $W = J(\psi)$ as in the definition of weak near-optimality, because we aim to compare different input states (for channel estimation) instead of different POVMs (for state estimation) and the cost matrix should not depend on the input state. $W = \mathbb{1}$ is the most natural choice as it assigns equal importance to all parameters.

up to a constant factor. Note that it is sufficient to consider only pure input states here because of the convexity of the CFIM. In Eq. (106), we also allow $\psi^{(i)}$ to be an entangled state (and M to be a correlated measurement) across the probe system and an arbitrarily large ancillary system as explained below.

• Maximally entangled states

In the first scenario, we make use of an ancillary system A, in which case the input state can be an entangled state between the original probe system P and the ancillary system. The Hamiltonian evolution acts only on the probe system, and the measurement can act on the joint system. Specifically, we choose the maximally entangled state as the input state, i.e.,

$$|\psi_{\text{PA}}^{\text{ME}}\rangle = \frac{1}{\sqrt{d}} \sum_{k=0}^{d-1} |k\rangle_{\text{P}} |k\rangle_{\text{A}}, \quad (107)$$

where $\{|k\rangle\}_{k=0}^{d-1}$ is the computational basis. The QFIM can be calculated through Eq. (101) where P_j are interpreted as $(P_j)_{\text{P}} \otimes \mathbb{1}_{\text{A}}$, and we have

$$J(\psi^{\text{ME}}) = 4\mathbb{1}, \text{ and } \text{Tr}(J(\psi^{\text{ME}})^{-1}) = \frac{d^2 - 1}{4}. \quad (108)$$

The deviation observable for each parameter is

$$X_j(\psi^{\text{ME}}; \theta) = \frac{i}{2} [|\psi_\theta^{\text{ME}}\rangle \langle \psi_\theta^{\text{ME}}|, P_j], \quad (109)$$

which induces the local shadow estimator that achieve the QFIM up to a constant factor via 3-design measurements. When θ is sufficiently close to zero, in order to estimate θ_j , it is sufficient to use $X_j(\psi^{\text{ME}}; (0, \dots, \theta_j, \dots, 0)) \approx X_j(\psi^{\text{ME}}; 0) + \theta_j \frac{d+1}{2d} [(P_j |\psi^{\text{ME}}\rangle \langle \psi^{\text{ME}}| - |\psi^{\text{ME}}\rangle \langle \psi^{\text{ME}}| P_j), P_j]$ as the deviation observable to estimate θ_j , where we set $\theta_{k \neq j} = 0$ because their influence on the local shadow estimator is second-order and we also ignore the $O(\theta_j^2)$ term. The corresponding local shadow estimator $\text{Tr}(X_j \hat{\rho}(s))$ is then efficiently computable when the 3-design measurement bases $|s\rangle$ are random stabilizer states using the property that $|\psi^{\text{ME}}\rangle$ is also a stabilizer state.

$|\psi^{\text{ME}}\rangle$ minimizes $\text{Tr}(J(\psi)^{-1})$, because for any ψ ,

$$\text{Tr}(J(\psi)^{-1}) \geq (d^2 - 1)^2 \text{Tr}(J(\psi^{\text{ME}})^{-1}) \geq \frac{d^2 - 1}{4}. \quad (110)$$

The above equalities hold when $\psi = \psi^{\text{ME}}$. The first inequality above is Cauchy-Schwarz and the second is due to $J(\psi) \leq Q(\psi)$ and

$$\text{Tr}(J(\psi)) \leq \text{Tr}(Q(\psi)) = 4(d^2 - 1), \quad (111)$$

for any input state ψ , where $Q_{jk} := 4\langle \psi | \frac{1}{2} \{P_j, P_k\} | \psi \rangle$. This implies

$$w \geq \frac{d^2 - 1}{4}, \quad (112)$$

because for any $\varepsilon > 0$, there exists an input state ensemble $\{p^{(i)}, \psi^{(i)}, M^{(i)}\}$ such that

$$\begin{aligned}
w + \varepsilon &\geq \text{Tr}(I(\{p^{(i)}, \psi^{(i)}, M^{(i)}\})^{-1}) \\
&= \text{Tr}\left(\left(\sum_i p^{(i)} I(\psi^{(i)}, M^{(i)})\right)^{-1}\right) \\
&\geq (d^2 - 1)^2 \left(\sum_i p^{(i)} \text{Tr}(I(\psi^{(i)}, M^{(i)}))\right)^{-1} \\
&\geq (d^2 - 1)^2 \left(\sum_i p^{(i)} \text{Tr}(J(\psi^{(i)}))\right)^{-1} \\
&\geq \frac{d^2 - 1}{4} = \text{Tr}(J(\psi^{\text{ME}})^{-1}), \tag{113}
\end{aligned}$$

where we use Eq. (103) in the second line, the Cauchy-Schwarz in the third line, the CRB $J(\psi^{(i)})^{-1} \preceq I(\psi^{(i)}, M^{(i)})^{-1}$ in the fourth line and Eq. (111) in the last line. Thus, ψ^{ME} is near-optimal for the Hamiltonian estimation problem. For any measurement M given by a 3-design,

$$\text{Tr}(I(\psi^{\text{ME}}, M)^{-1}) \leq 4\text{Tr}(J(\psi^{\text{ME}})^{-1}) \leq 4w, \tag{114}$$

where we use Theorem 1 to show the first inequality.

• Random stabilizer states

In the second scenario, we consider ancilla-free scenarios, which is more favorable in practice because the ancillary system is not always available. An input state ensemble is necessary here because with a single input state, at most $d - 1$ number of parameters can be estimated. Here we choose

$$p^{\text{C},(i)} = \frac{1}{|\mathcal{U}|}, \quad |\psi^{\text{C},(i)}\rangle = U^{(i)} |0^{\otimes n}\rangle, \tag{115}$$

where $U^{(i)}$ is an element from the random Clifford unitary ensemble \mathcal{U} . Let the joint state on the fictitious reference system R and the probe system P be

$$\rho_{\text{RP}}^{\text{C}} = \frac{1}{|\mathcal{U}|} \sum_i |i\rangle \langle i|_{\text{R}} \otimes \psi^{\text{C},(i)}. \tag{116}$$

Then

$$\begin{aligned}
J(\rho_{\text{RP}}^{\text{C}}) &= \sum_i p^{\text{C},(i)} J(\psi^{\text{C},(i)})_{jk} \tag{117} \\
&= 4 \left(\delta_{jk} - \frac{\delta_{jk}}{d+1} \right) = \frac{4d\delta_{jk}}{d+1}, \tag{118}
\end{aligned}$$

where we use

$$\begin{aligned}
\mathbb{E}_i[\langle \psi^{\text{C},(i)} | \frac{1}{2} \{P_j, P_k\} | \psi^{\text{C},(i)} \rangle] &= \frac{1}{d} \text{Tr}\left(\frac{1}{2} \{P_j, P_k\}\right), \\
\mathbb{E}_i[\langle \psi^{\text{C},(i)} | P_j | \psi^{\text{C},(i)} \rangle \langle \psi^{\text{C},(i)} | P_k | \psi^{\text{C},(i)} \rangle] &= \frac{\text{Tr}(P_j P_k)}{d(d+1)}.
\end{aligned}$$

These are properties of random Clifford unitaries as a 1-design and a 2-design. For any measurement M given by a 3-design,

$$\begin{aligned}
&\text{Tr}(I(\{p^{\text{C},(i)}, \psi^{\text{C},(i)}, M\})^{-1}) \\
&\leq 4\text{Tr}\left(\left(\sum_i p^{\text{C},(i)} J(\psi^{\text{C},(i)})\right)^{-1}\right) \\
&= \frac{(d+1)}{d} (d^2 - 1) \leq \frac{4(d+1)}{d} w, \tag{119}
\end{aligned}$$

where we use Eq. (103) and Theorem 1 to show the first inequality and Eq. (112) and Eq. (118) in the second step.

For input states chosen randomly from a state ensemble, we define the deviation observable for each parameter as

$$X_j(\psi^{\text{C},(i)}; \theta) = \sum_k (J(\rho_{\text{RP}}^{\text{C}})^{-1})_{jk} L_k(\psi^{\text{C},(i)}) \tag{120}$$

$$= \frac{i(d+1)}{2d} [|\psi_{\theta}^{\text{C},(i)}\rangle \langle \psi_{\theta}^{\text{C},(i)}|, P_j]. \tag{121}$$

They induce the following local shadow estimator (at θ^0) as a generalization of Eq. (37) to the case of random input states,

$$\hat{\theta}_j(s; i, \theta^0) = \theta_j^0 + \text{Tr}((X_j(\psi^{\text{C},(i)}; \theta)|_{\theta=\theta^0}) \hat{\rho}(s)). \tag{122}$$

It is a function of both i and θ^0 where the index i of the choice of the input state that is known to the experimenter. The overall variance V in this case is the average of the variance for different input states, which is given by

$$\begin{aligned}
(J_{\text{RP}} V J_{\text{RP}})_{jk} &= \frac{d+1}{d+2} \mathbb{E}_i \left[\text{Tr}(L_j^{\text{C},(i)} L_k^{\text{C},(i)}) \right. \\
&\quad \left. + \text{Tr}(\psi_{\theta}^{\text{C},(i)} \{L_j^{\text{C},(i)}, L_k^{\text{C},(i)}\}) \right] \\
&= \frac{d+1}{4(d+2)} \mathbb{E}_i [J(\psi^{\text{C},(i)})] = \frac{d+1}{4(d+2)} J_{\text{RP}}, \tag{123}
\end{aligned}$$

where J_{RP} is the shorthand of the averaged QFIM $J(\rho_{\text{RP}}^{\text{C}})$. The above shows how the local shadow estimators achieve the near-optimal performance and the derivation follows exactly from the proof of Theorem 1 after taking random inputs into consideration.

To summarize, the discussion above (in particular, Eq. (114) and Eq. (119)) implies the following corollary of Theorem 1:

Corollary 1. *The maximally entangled state, or the random stabilizer state ensemble, together with any 3-design measurement, forms a near-optimal protocol for the Hamiltonian estimation problem in Eq. (99) at $\theta = 0$.*

2. Noisy case

Using Theorem 2, the above discussions can be generalized to the situations where quantum noise affects the

Hamiltonian estimation. We assume a Pauli noise channel, in which case the parameterized quantum channel acting on the probe system P becomes

$$\mathcal{E}_\theta(\cdot) = (1-q)U_\theta(\cdot)U_\theta^\dagger + \sum_{k=1}^{d^2-1} q_k P_k U_\theta(\cdot)U_\theta^\dagger P_k, \quad (124)$$

where q_k are the probabilities of Pauli error P_k which sum up to the total noise rate q , and $q < 1/2$. We also define $q_0 := 1 - q$ and $P_0 = \mathbb{1}$ for future use. Again, we consider parameter estimation at $\theta = 0$. We will show that the maximally entangled state and the random stabilizer state ensemble can still achieve the optimal WMSE in the noiseless case (Eq. (106)) up to a constant factor that depends only on q .

• Maximally entangled states

In the first ancilla-assisted scenario, we have the maximally entangled state (Eq. (107)) as the input state. We assume no noise on the ancillary system. Then $(P_k \otimes \mathbb{1})|\psi^{\text{ME}}\rangle$ are orthogonal to each other for different k . (Below we omit $\otimes \mathbb{1}$ for simplicity.) Let Π be the rank-one projector onto $|\psi_\theta^{\text{ME}}\rangle := U_\theta |\psi^{\text{ME}}\rangle$, which is the eigenstate of the output state $\mathcal{E}_\theta(\psi^{\text{ME}})$ with the largest eigenvalue, and the probability of post-selecting on subspace Π_\perp is $\text{Tr}(\Pi_\perp \mathcal{E}_\theta(\psi)) = q$. The QFIM after post-selecting on Π_\perp satisfies

$$\begin{aligned} J^\perp(\psi^{\text{ME}}) &:= J \left[\sum_{k=1}^{d^2-1} \frac{q_k}{q} P_k U_\theta \psi^{\text{ME}} U_\theta^\dagger P_k \right] \\ &\succeq \sum_{k=1}^{d^2-1} \frac{q_k}{q} J[P_k U_\theta \psi^{\text{ME}} U_\theta^\dagger P_k] = J[\psi_\theta^{\text{ME}}] = 4\mathbb{1}, \end{aligned} \quad (125)$$

where we use the convexity of the QFIM in the first inequality, $J[P_k \psi_\theta^{\text{ME}} P_k] = J[\psi_\theta^{\text{ME}}]$ in the second equality. Here, we use $J[\star]$ to denote the QFIM of state \star , and thus $J(\star) = J[\mathcal{E}_\theta(\star)]$ by definition. (Previously, the dependence of J on the parameterized states was implicit, as these states were always straightforwardly ρ_θ or ψ_θ . However, in the current context involving multiple distinct parameterized states, it is necessary to explicitly indicate this dependence.) Meanwhile, the QFIM of the output state $\mathcal{E}_\theta(\psi^{\text{ME}})$ is

$$\begin{aligned} J(\psi^{\text{ME}})_{ij} &:= J \left[\sum_{k=0}^{d^2-1} q_k P_k U_\theta \psi^{\text{ME}} U_\theta^\dagger P_k \right]_{ij} \\ &= 2\delta_{ij} \sum_{\substack{0 \leq k \leq d^2-1, \\ q_k + q_{k+i} > 0}} \frac{|q_{k+i} - q_k|^2}{q_k + q_{k+i}}. \end{aligned} \quad (126)$$

Note that the $+$ sign in q_{k+i} should be interpreted in the following way: q_{k+i} denotes the noise rate of the Pauli operator $P_{k+i} \propto \eta_{k,i} P_k P_i$. The derivation of Eq. (126)

can be found in Appx. F. Then

$$J(\psi^{\text{ME}})_{ij} \geq 4\delta_{ij} \frac{|q_i - q_0|^2}{q_0 + q_i} \geq 4\delta_{ij}(1-2q)^2, \quad (127)$$

where we use $q_i \leq q$ in the last step. Combining Eq. (125) and Eq. (127), we have

$$J(\psi^{\text{ME}}) - qJ^\perp(\psi^{\text{ME}}) \succeq \frac{(1-2q)^2 - q}{(1-2q)^2} J(\psi^{\text{ME}}). \quad (128)$$

This means the noisy output state $\mathcal{E}_\theta(\psi^{\text{ME}})$ is a $(1 - q, \frac{(1-2q)^2 - q}{(1-2q)^2})$ -approximately low-rank well-conditioned state, according to Definition 3. Applying Theorem 2, we know when M is given by a 3-design,

$$\begin{aligned} I(\psi^{\text{ME}}, M) &\succeq \frac{d+2}{d+1} \frac{(1-q)^2(1-4q)}{2(2-q)(1-2q)^2} J(\psi^{\text{ME}}) \\ &\succeq \frac{d+2}{d+1} \frac{(1-q)^2(1-4q)}{2(2-q)} (4\mathbb{1}), \end{aligned} \quad (129)$$

where $J(\psi^{\text{ME}})$ is the QFIM with the maximally entangled state as the input state for the noisy Hamiltonian estimation problem and $4\mathbb{1}$ is the QFIM of the maximally entangled input state in the noiseless case.

We can also calculate the deviation observable for each parameter (Eq. (55)). Using

$$\tilde{L}_j(\psi_{\text{ME}}) = \frac{2i(q_0 - q_j)}{q_0 + q_j} [|\psi_\theta^{\text{ME}}\rangle \langle \psi_\theta^{\text{ME}}|, P_j \otimes \mathbb{1}_A], \quad (130)$$

$$\tilde{J}_{jk}(\psi_{\text{ME}}) = \frac{4(q_0 - q_j)^2}{(q_0 + q_j)^2} \delta_{jk}. \quad (131)$$

we have

$$X_j(\psi_{\text{ME}}; \theta) = \frac{i(q_0 + q_j)}{2(q_0 - q_j)} [|\psi_\theta^{\text{ME}}\rangle \langle \psi_\theta^{\text{ME}}|, P_j], \quad (132)$$

which is proportional to the deviation observable in the noiseless case (Eq. (109)). The simplification stems from the proof of Theorem 2 where we show the sufficiency to achieve near-optimal estimation by excluding the Π_\perp component in the SLD operators.

• Random stabilizer states

In the second ancilla-free scenario, we use the random stabilizer state ensemble (Eq. (115)). We first consider the special case where the input state is $|\psi^{C,(0)}\rangle := |0^{\otimes n}\rangle$. Let $|\psi_\theta^{C,(0)}\rangle := U_\theta |0^{\otimes n}\rangle$. Let Π be the rank-one projector onto $U_\theta |0^{\otimes n}\rangle$, and $\Pi^\perp = \mathbb{1} - \Pi$. The probability of post-selecting on subspace Π_\perp is

$$\text{Tr}(\Pi_\perp \mathcal{E}_\theta(\psi^{C,(0)})) = \sum_{k: \tilde{k} \neq 0^n} q_k =: \tilde{q} \leq q, \quad (133)$$

where we define \tilde{k} to be an n -bit string where \tilde{k}_i is equal to 1 if P_k on the i -th qubit is σ_x or σ_y , and \tilde{k}_i is equal to

0 if P_k on the i -th qubit is σ_z or $\mathbb{1}$. We also have

$$J^\perp(\psi^{C,(0)}) := J \left[\sum_{k:\bar{k} \neq 0^n} \frac{q_k}{\bar{q}} P_k U_\theta \psi^{C,(0)} U_\theta^\dagger P_k \right] \preceq J[\psi_\theta^{C,(0)}]. \quad (134)$$

We show in [Appx. G](#) that

$$J(\psi^{C,(0)}) - \tilde{q} J^\perp(\psi^{C,(0)}) \succeq \frac{(1-2q)^2 - q}{(1-2q)^2} J(\psi^{C,(0)}), \quad (135)$$

which indicates that the noisy output state $\mathcal{E}_\theta(\psi^{C,(0)})$ is a $(1 - q, \frac{(1-2q)^2 - q}{(1-2q)^2})$ -approximately low-rank well-conditioned state. Note that when we use an input state $|\psi^{C,(i)}\rangle := U^{(i)} |0^{\otimes n}\rangle$ where $U^{(i)}$ is a Clifford unitary, we have

$$\mathcal{E}_\theta(\psi^{C,(i)}) = U^{(i)} \mathcal{E}'_\theta(\psi^{C,(0)}) U^{(i)\dagger}, \quad (136)$$

where \mathcal{E}'_θ is equal to \mathcal{E}_θ with all Pauli operators P_k , both in the noise channel and the Hamiltonian evolution, replaced by $U^{(i)\dagger} P_k U^{(i)}$. [Eq. \(135\)](#) still holds under such a replacement, and we conclude that $\mathcal{E}_\theta(\psi^{C,(i)})$ are $(1 - q, \frac{(1-2q)^2 - q}{(1-2q)^2})$ -approximately low-rank well-conditioned states for all i 's. Applying [Theorem 2](#), we know when M is given by a 3-design,

$$I(\psi^{C,(i)}, M) \succeq \frac{d+2}{d+1} \frac{(1-q)^2(1-4q)}{2(2-q)(1-2q)^2} J(\psi^{C,(i)}). \quad (137)$$

Then

$$\begin{aligned} I(\{p^{C,(i)}, \psi^{C,(i)}, \tilde{M}\}) &= \sum_i p^{C,(i)} I(\psi^{C,(i)}, M) \\ &\succeq \frac{d+2}{d+1} \frac{(1-q)^2(1-4q)}{2(2-q)(1-2q)^2} \sum_i p^{C,(i)} J(\psi^{C,(i)}) \\ &\succeq \frac{d+2}{d+1} \frac{(1-q)^2(1-4q)}{2(2-q)} \left(\frac{4d}{d+1} \mathbb{1} \right), \end{aligned} \quad (138)$$

where the last line is proved in [Appx. G](#). The deviation observables in this case may not have simple expressions (see discussion in [Appx. G](#)).

To summarize, the discussion above (in particular, [Eq. \(129\)](#) and [Eq. \(138\)](#)) shows the near-optimality of the maximally entangled state and the random stabilizer state ensemble when q is sufficiently small. We have the following corollary of [Theorem 2](#).

Corollary 2. *The maximally entangled state, or the random stabilizer state ensemble, together with any 3-design measurement, forms a near-optimal protocol for the Hamiltonian estimation problem in [Eq. \(99\)](#) at $\theta = 0$, even under the influence of sufficiently small Pauli noise.*

VIII. CONCLUSIONS AND OUTLOOK

In this work, we showed randomized measurements are near-optimal for pure states and approximately low-rank

well-conditioned states, and are weakly near-optimal for three families of rank- r well-conditioned states. We also provide examples where randomized measurements are explicitly shown to be useful or proved to be suboptimal.

Our work not only establishes randomized measurements are an important tool in multi-parameter quantum metrology but also highlights several open problems and new research directions. First, although we classified several important families of quantum states for which randomized measurements have the near-optimal performance, it still remains largely open in general which types of mixed states can be estimated with randomized measurements (weakly) near-optimally. Second, we mostly analyze quantum measurements given by 3-designs and it is desirable to understand the performance of other types of randomized measurements that are even more experimentally friendly, e.g., tensor product of single-qudit 3-designs (i.e., Pauli measurements in the qubit case), or approximate 3-designs (which can be implemented in log-depth circuits [\[88\]](#)). Third, it will be interesting to study generalization of our results to quantum channel estimation, instead of quantum state estimation, with optimization of input states also taken into consideration. Finally, our discussion is mostly restricted to local parameter estimation, and it is interesting to consider generalization to global parameter estimation, using e.g., Bayesian approach [\[109\]](#) and hypothesis testing approach [\[110\]](#).

DATA AVAILABILITY

Codes and data for this project are available at the following Github repository: <https://github.com/csenrui/random-measurement-metrology>.

ACKNOWLEDGMENTS

We would like to thank Hsin-Yuan Huang for helpful discussions. S.Z. acknowledges support from Perimeter Institute for Theoretical Physics, a research institute supported in part by the Government of Canada through the Department of Innovation, Science and Economic Development Canada and by the Province of Ontario through the Ministry of Colleges and Universities. S.C. acknowledges support from ARO (W911NF-23-1-0077), AFOSR MURI (FA9550-21-1-0209), NTT Research, and the Institute for Quantum Information and Matter, an NSF Physics Frontiers Center (NSF Grant PHY-2317110). S.C. thanks Perimeter Institute for their hospitality where part of this work was completed.

- [1] V. Giovannetti, S. Lloyd, and L. Maccone, Advances in quantum metrology, *Nat. Photonics*. **5**, 222 (2011).
- [2] C. L. Degen, F. Reinhard, and P. Cappellaro, Quantum sensing, *Rev. Mod. Phys.* **89**, 035002 (2017).
- [3] L. Pezzè, A. Smerzi, M. K. Oberthaler, R. Schmied, and P. Treutlein, Quantum metrology with nonclassical states of atomic ensembles, *Rev. Mod. Phys.* **90**, 035005 (2018).
- [4] S. Pirandola, B. R. Bardhan, T. Gehring, C. Weedbrook, and S. Lloyd, Advances in photonic quantum sensing, *Nat. Photonics*. **12**, 724 (2018).
- [5] C. M. Caves, Quantum-mechanical noise in an interferometer, *Phys. Rev. D* **23**, 1693 (1981).
- [6] B. Yurke, S. L. McCall, and J. R. Klauder, $Su(2)$ and $su(1,1)$ interferometers, *Phys. Rev. A* **33**, 4033 (1986).
- [7] LIGO Collaboration, A gravitational wave observatory operating beyond the quantum shot-noise limit, *Nat. Phys.* **7**, 962 (2011).
- [8] LIGO Collaboration, Enhanced sensitivity of the LIGO gravitational wave detector by using squeezed states of light, *Nat. Photonics*. **7**, 613 (2013).
- [9] D. J. Wineland, J. J. Bollinger, W. M. Itano, F. L. Moore, and D. J. Heinzen, Spin squeezing and reduced quantum noise in spectroscopy, *Phys. Rev. A* **46**, R6797 (1992).
- [10] J. J. Bollinger, W. M. Itano, D. J. Wineland, and D. J. Heinzen, Optimal frequency measurements with maximally correlated states, *Phys. Rev. A* **54**, R4649 (1996).
- [11] D. Leibfried, M. D. Barrett, T. Schaetz, J. Britton, J. Chiaverini, W. M. Itano, J. D. Jost, C. Langer, and D. J. Wineland, Toward Heisenberg-limited spectroscopy with multiparticle entangled states, *Science* **304**, 1476 (2004).
- [12] J. Taylor, P. Cappellaro, L. Childress, L. Jiang, D. Budker, P. Hemmer, A. Yacoby, R. Walsworth, and M. Lukin, High-sensitivity diamond magnetometer with nanoscale resolution, *Nat. Phys.* **4**, 810 (2008).
- [13] H. Zhou, J. Choi, S. Choi, R. Landig, A. M. Douglas, J. Isoya, F. Jelezko, S. Onoda, H. Sumiya, P. Cappellaro, *et al.*, Quantum metrology with strongly interacting spin systems, *Phys. Rev. X* **10**, 031003 (2020).
- [14] T. Rosenband, D. Hume, P. Schmidt, C.-W. Chou, A. Brusch, L. Lorini, W. Oskay, R. E. Drullinger, T. M. Fortier, J. E. Stalnaker, *et al.*, Frequency ratio of Al^+ and Hg^+ single-ion optical clocks; metrology at the 17th decimal place, *Science* **319**, 1808 (2008).
- [15] J. Appel, P. J. Windpassinger, D. Oblak, U. B. Hoff, N. Kjærgaard, and E. S. Polzik, Mesoscopic atomic entanglement for precision measurements beyond the standard quantum limit, *Proc. Natl. Acad. Sci.* **106**, 10960 (2009).
- [16] A. D. Ludlow, M. M. Boyd, J. Ye, E. Peik, and P. O. Schmidt, Optical atomic clocks, *Rev. Mod. Phys.* **87**, 637 (2015).
- [17] R. Kaubruegger, D. V. Vasilyev, M. Schulte, K. Hammerer, and P. Zoller, Quantum variational optimization of Ramsey interferometry and atomic clocks, *Phys. Rev. X* **11**, 041045 (2021).
- [18] C. D. Marciniak, T. Feldker, I. Pogorelov, R. Kaubruegger, D. V. Vasilyev, R. van Bijnen, P. Schindler, P. Zoller, R. Blatt, and T. Monz, Optimal metrology with programmable quantum sensors, *Nature* **603**, 604 (2022).
- [19] D. Le Sage, K. Arai, D. R. Glenn, S. J. DeVience, L. M. Pham, L. Rahn-Lee, M. D. Lukin, A. Yacoby, A. Komeili, and R. L. Walsworth, Optical magnetic imaging of living cells, *Nature* **496**, 486 (2013).
- [20] G. B. Lemos, V. Borish, G. D. Cole, S. Ramelow, R. Lapkiewicz, and A. Zeilinger, Quantum imaging with undetected photons, *Nature* **512**, 409 (2014).
- [21] M. Tsang, R. Nair, and X.-M. Lu, Quantum theory of superresolution for two incoherent optical point sources, *Phys. Rev. X* **6**, 031033 (2016).
- [22] M. Abobeih, J. Randall, C. Bradley, H. Bartling, M. Bakker, M. Degen, M. Markham, D. Twitchen, and T. Taminiau, Atomic-scale imaging of a 27-nuclear-spin cluster using a quantum sensor, *Nature* **576**, 411 (2019).
- [23] C. W. Helstrom, Minimum mean-squared error of estimates in quantum statistics, *Phys. Lett. A* **25**, 101 (1967).
- [24] C. W. Helstrom, The minimum variance of estimates in quantum signal detection, *IEEE Trans. Inf. Theory* **14**, 234 (1968).
- [25] C. W. Helstrom, *Quantum detection and estimation theory* (Academic press, 1976).
- [26] A. S. Holevo, *Probabilistic and statistical aspects of quantum theory*, Vol. 1 (Springer Science & Business Media, 2011).
- [27] S. L. Braunstein and C. M. Caves, Statistical distance and the geometry of quantum states, *Phys. Rev. Lett.* **72**, 3439 (1994).
- [28] O. E. Barndorff-Nielsen and R. D. Gill, Fisher information in quantum statistics, *J. Phys. A: Math. Gen.* **33**, 4481 (2000).
- [29] M. G. Paris, Quantum estimation for quantum technology, *Int. J. Quantum Inf.* **7**, 125 (2009).
- [30] R. D. Gill and S. Massar, State estimation for large ensembles, *Physical Review A* **61**, 042312 (2000).
- [31] K. Matsumoto, A new approach to the Cramér-Rao-type bound of the pure-state model, *Journal of Physics A: Mathematical and General* **35**, 3111 (2002).
- [32] H. Nagaoka, A new approach to cramer-rao bounds for quantum state estimation, in *Asymptotic theory of quantum statistical inference: Selected Papers* (World Scientific, 2005) pp. 100–112.
- [33] L. O. Conlon, J. Suzuki, P. K. Lam, and S. M. Assad, Efficient computation of the nagaoka-hayashi bound for multiparameter estimation with separable measurements, *npj Quantum Information* **7**, 110 (2021).
- [34] S. Ragy, M. Jarzyna, and R. Demkowicz-Dobrzański, Compatibility in multiparameter quantum metrology, *Physical Review A* **94**, 052108 (2016).
- [35] R. Demkowicz-Dobrzański, W. Górecki, and M. Guţă, Multi-parameter estimation beyond quantum fisher information, *Journal of Physics A: Mathematical and Theoretical* **53**, 363001 (2020).
- [36] M. Szczykulska, T. Baumgratz, and A. Datta, Multiparameter quantum metrology, *Advances in Physics: X* **1**, 621 (2016).
- [37] J. Liu, H. Yuan, X.-M. Lu, and X. Wang, Quantum fisher information matrix and multiparameter estimation, *Journal of Physics A: Mathematical and Theoret-*

- ical **53**, 023001 (2020).
- [38] J. S. Sidhu and P. Kok, Geometric perspective on quantum parameter estimation, *AVS Quantum Science* **2** (2020).
- [39] J. Kahn and M. Guță, Local asymptotic normality for finite dimensional quantum systems, *Communications in Mathematical Physics* **289**, 597 (2009).
- [40] K. Yamagata, A. Fujiwara, and R. D. Gill, Quantum local asymptotic normality based on a new quantum likelihood ratio, *The Annals of Statistics* **41**, 2197 (2013).
- [41] Y. Yang, G. Chiribella, and M. Hayashi, Attaining the ultimate precision limit in quantum state estimation, *Communications in Mathematical Physics* **368**, 223 (2019).
- [42] P. C. Humphreys, M. Barbieri, A. Datta, and I. A. Walmsley, Quantum enhanced multiple phase estimation, *Physical Review Letters* **111**, 070403 (2013).
- [43] M. D. Vidrighin, G. Donati, M. G. Genoni, X.-M. Jin, W. S. Kolthammer, M. Kim, A. Datta, M. Barbieri, and I. A. Walmsley, Joint estimation of phase and phase diffusion for quantum metrology, *Nature Communications* **5**, 3532 (2014).
- [44] J. Suzuki, Explicit formula for the holevo bound for two-parameter qubit-state estimation problem, *Journal of Mathematical Physics* **57** (2016).
- [45] Y. Chen and H. Yuan, Maximal quantum fisher information matrix, *New Journal of Physics* **19**, 063023 (2017).
- [46] L. Pezzè, M. A. Ciampini, N. Spagnolo, P. C. Humphreys, A. Datta, I. A. Walmsley, M. Barbieri, F. Sciarrino, and A. Smerzi, Optimal measurements for simultaneous quantum estimation of multiple phases, *Physical Review Letters* **119**, 130504 (2017).
- [47] N. Li, C. Ferrie, J. A. Gross, A. Kalev, and C. M. Caves, Fisher-symmetric informationally complete measurements for pure states, *Physical Review Letters* **116**, 180402 (2016).
- [48] H. Zhu and M. Hayashi, Universally fisher-symmetric informationally complete measurements, *Physical Review Letters* **120**, 030404 (2018).
- [49] C. Vargas, L. Pereira, and A. Delgado, Near-optimal pure state estimation with adaptive fisher-symmetric measurements, *arXiv:2412.04555* (2024).
- [50] J. Yang, S. Pang, Y. Zhou, and A. N. Jordan, Optimal measurements for quantum multiparameter estimation with general states, *Physical Review A* **100**, 032104 (2019).
- [51] A. Carollo, B. Spagnolo, A. A. Dubkov, and D. Valenti, On quantumness in multi-parameter quantum estimation, *Journal of Statistical Mechanics: Theory and Experiment* **2019**, 094010 (2019).
- [52] F. Albarelli, M. Barbieri, M. G. Genoni, and I. Gianani, A perspective on multiparameter quantum metrology: From theoretical tools to applications in quantum imaging, *Physics Letters A* **384**, 126311 (2020).
- [53] J. Suzuki, Y. Yang, and M. Hayashi, Quantum state estimation with nuisance parameters, *Journal of Physics A: Mathematical and Theoretical* **53**, 453001 (2020).
- [54] Z. Hou, Z. Zhang, G.-Y. Xiang, C.-F. Li, G.-C. Guo, H. Chen, L. Liu, and H. Yuan, Minimal tradeoff and ultimate precision limit of multiparameter quantum magnetometry under the parallel scheme, *Physical Review Letters* **125**, 020501 (2020).
- [55] F. Belliardo and V. Giovannetti, Incompatibility in quantum parameter estimation, *New Journal of Physics* **23**, 063055 (2021).
- [56] A. Candeloro, M. G. Paris, and M. G. Genoni, On the properties of the asymptotic incompatibility measure in multiparameter quantum estimation, *Journal of Physics A: Mathematical and Theoretical* **54**, 485301 (2021).
- [57] X.-M. Lu and X. Wang, Incorporating heisenberg's uncertainty principle into quantum multiparameter estimation, *Physical Review Letters* **126**, 120503 (2021).
- [58] H. Chen, Y. Chen, and H. Yuan, Information geometry under hierarchical quantum measurement, *Physical Review Letters* **128**, 250502 (2022).
- [59] H. Chen, Y. Chen, and H. Yuan, Incompatibility measures in multiparameter quantum estimation under hierarchical quantum measurements, *Physical Review A* **105**, 062442 (2022).
- [60] S. K. Yung, L. O. Conlon, J. Zhao, P. K. Lam, and S. M. Assad, Comparison of estimation limits for quantum two-parameter estimation, *Physical Review Research* **6**, 033315 (2024).
- [61] F. Albarelli, J. F. Friel, and A. Datta, Evaluating the holevo Cramér-Rao bound for multiparameter quantum metrology, *Physical Review Letters* **123**, 200503 (2019).
- [62] W. Górecki, S. Zhou, L. Jiang, and R. Demkowicz-Dobrzański, Optimal probes and error-correction schemes in multi-parameter quantum metrology, *Quantum* **4**, 288 (2020).
- [63] M. Tsang, F. Albarelli, and A. Datta, Quantum semi-parametric estimation, *Physical Review X* **10**, 031023 (2020).
- [64] J. S. Sidhu, Y. Ouyang, E. T. Campbell, and P. Kok, Tight bounds on the simultaneous estimation of incompatible parameters, *Physical Review X* **11**, 011028 (2021).
- [65] M. Hayashi and Y. Ouyang, Tight Cramér-Rao type bounds for multiparameter quantum metrology through conic programming, *Quantum* **7**, 1094 (2023).
- [66] J. W. Gardner, T. Gefen, S. A. Haine, J. J. Hope, and Y. Chen, Achieving the fundamental quantum limit of linear waveform estimation, *Physical Review Letters* **132**, 130801 (2024).
- [67] A. Elben, S. T. Flammia, H.-Y. Huang, R. Kueng, J. Preskill, B. Vermersch, and P. Zoller, The randomized measurement toolbox, *Nature Reviews Physics* **5**, 9 (2023).
- [68] J. Watrous, *The theory of quantum information* (Cambridge university press, 2018).
- [69] E. Knill, D. Leibfried, R. Reichle, J. Britton, R. B. Blakestad, J. D. Jost, C. Langer, R. Ozeri, S. Seidelin, and D. J. Wineland, Randomized benchmarking of quantum gates, *Physical Review A* **77**, 012307 (2008).
- [70] C. Dankert, R. Cleve, J. Emerson, and E. Livine, Exact and approximate unitary 2-designs and their application to fidelity estimation, *Physical Review A* **80**, 012304 (2009).
- [71] J. Emerson, R. Alicki, and K. Życzkowski, Scalable noise estimation with random unitary operators, *Journal of Optics B: Quantum and Semiclassical Optics* **7**, S347 (2005).
- [72] H.-Y. Huang, R. Kueng, and J. Preskill, Predicting many properties of a quantum system from very few measurements, *Nature Physics* **16**, 1050 (2020).
- [73] T. Brydges, A. Elben, P. Jurcevic, B. Vermersch, C. Maier, B. P. Lanyon, P. Zoller, R. Blatt, and C. F. Roos, Probing rényi entanglement entropy via random-

- ized measurements, *Science* **364**, 260 (2019).
- [74] J. M. Renes, R. Blume-Kohout, A. J. Scott, and C. M. Caves, Symmetric informationally complete quantum measurements, *Journal of Mathematical Physics* **45**, 2171 (2004).
- [75] A. Ambainis and J. Emerson, Quantum t-designs: t-wise independence in the quantum world, in *Twenty-Second Annual IEEE Conference on Computational Complexity (CCC'07)* (IEEE, 2007) pp. 129–140.
- [76] A. Roy and A. J. Scott, Unitary designs and codes, *Designs, codes and cryptography* **53**, 13 (2009).
- [77] D. Gross, K. Audenaert, and J. Eisert, Evenly distributed unitaries: On the structure of unitary designs, *Journal of mathematical physics* **48** (2007).
- [78] R. Kueng and D. Gross, Qubit stabilizer states are complex projective 3-designs, arXiv:1510.02767 (2015).
- [79] Z. Webb, The clifford group forms a unitary 3-design, *Quantum Information and Computation* **16**, 1379 (2016).
- [80] H. Zhu, Multiqubit clifford groups are unitary 3-designs, *Physical Review A* **96**, 062336 (2017).
- [81] S. Aaronson and D. Gottesman, Improved simulation of stabilizer circuits, *Physical Review A* **70**, 052328 (2004).
- [82] S. Bravyi and D. Maslov, Hadamard-free circuits expose the structure of the clifford group, *IEEE Transactions on Information Theory* **67**, 4546 (2021).
- [83] C. Moore and M. Nilsson, Parallel quantum computation and quantum codes, *SIAM journal on computing* **31**, 799 (2001).
- [84] J. Jiang, X. Sun, S.-H. Teng, B. Wu, K. Wu, and J. Zhang, Optimal space-depth trade-off of cnot circuits in quantum logic synthesis, in *Proceedings of the Fourteenth Annual ACM-SIAM Symposium on Discrete Algorithms* (SIAM, 2020) pp. 213–229.
- [85] F. G. Brandao, A. W. Harrow, and M. Horodecki, Local random quantum circuits are approximate polynomial-designs, *Communications in Mathematical Physics* **346**, 397 (2016).
- [86] J. Haferkamp, F. Montealegre-Mora, M. Heinrich, J. Eisert, D. Gross, and I. Roth, Efficient unitary designs with a system-size independent number of non-clifford gates, *Communications in Mathematical Physics* **397**, 995 (2023).
- [87] A. W. Harrow and S. Mehraban, Approximate unitary t-designs by short random quantum circuits using nearest-neighbor and long-range gates, *Communications in Mathematical Physics* **401**, 1531 (2023).
- [88] T. Schuster, J. Haferkamp, and H.-Y. Huang, Random unitaries in extremely low depth, *Science* **389**, 92 (2025).
- [89] B. Bajnok, Constructions of spherical 3-designs, *Graphs and Combinatorics* **14**, 97 (1998).
- [90] E. Bannai, M. Nakahara, D. Zhao, and Y. Zhu, On the explicit constructions of certain unitary t-designs, *Journal of Physics A: Mathematical and Theoretical* **52**, 495301 (2019).
- [91] E. Bannai, Y. Nakata, T. Okuda, and D. Zhao, Explicit construction of exact unitary designs, *Advances in Mathematics* **405**, 108457 (2022).
- [92] C. R. Rao, C. R. Rao, M. Statistiker, C. R. Rao, and C. R. Rao, *Linear statistical inference and its applications*, Vol. 2 (Wiley New York, 1973).
- [93] S. M. Kay, *Fundamentals of statistical signal processing: Volume I Estimation theory* (Prentice-Hall, Inc., 1993).
- [94] E. L. Lehmann and G. Casella, *Theory of point estimation* (Springer Science & Business Media, 2006).
- [95] D. R. Cox, *Inference and asymptotics* (Routledge, 2017).
- [96] G. Casella and R. L. Berger, *Statistical inference*, Vol. 2 (Duxbury Pacific Grove, CA, 2002).
- [97] S. Chen, J. Cotler, H.-Y. Huang, and J. Li, Exponential separations between learning with and without quantum memory, in *2021 IEEE 62nd Annual Symposium on Foundations of Computer Science (FOCS)* (IEEE, 2022) pp. 574–585.
- [98] M. A. Nielsen and I. L. Chuang, *Quantum Computation and Quantum Information* (Cambridge University Press, 2010).
- [99] H. Nagaoka, On the parameter estimation problem for quantum statistical models, in *Asymptotic Theory Of Quantum Statistical Inference: Selected Papers* (World Scientific, 2005) pp. 125–132.
- [100] Z. Hou, J.-F. Tang, J. Shang, H. Zhu, J. Li, Y. Yuan, K.-D. Wu, G.-Y. Xiang, C.-F. Li, and G.-C. Guo, Deterministic realization of collective measurements via photonic quantum walks, *Nature communications* **9**, 1414 (2018).
- [101] M. Hayashi, Asymptotic estimation theory for a finite-dimensional pure state model, *Journal of Physics A: Mathematical and General* **31**, 4633 (1998).
- [102] H. Zhu, Quantum state estimation and symmetric informationally complete poms (2012), available online at <http://scholarbank.nus.edu.sg/bitstream/10635/35247/1/ZhuHJthesis.pdf>.
- [103] H. Zhu, Quantum state estimation with informationally overcomplete measurements, *Physical Review A* **90**, 012115 (2014).
- [104] J. Lu and K. Sha, Quantum fisher information matrix via its classical counterpart from random measurements, arXiv preprint arXiv:2509.08196 (2025).
- [105] D. A. Roberts and B. Yoshida, Chaos and complexity by design, *Journal of High Energy Physics* **2017**, 1 (2017).
- [106] B. Efron and R. J. Tibshirani, *An introduction to the bootstrap* (Chapman and Hall/CRC, 1994).
- [107] J. L. Hintze and R. D. Nelson, Violin plots: a box plot-density trace synergism, *The American Statistician* **52**, 181 (1998).
- [108] A. Javadi-Abhari, M. Treinish, K. Krsulich, C. J. Wood, J. Lishman, J. Gacon, S. Martiel, P. D. Nation, L. S. Bishop, A. W. Cross, *et al.*, Quantum computing with Qiskit, arXiv preprint arXiv:2405.08810 (2024).
- [109] W. Górecki, R. Demkowicz-Dobrzański, H. M. Wiseman, and D. W. Berry, π -corrected Heisenberg limit, *Phys. Rev. Lett.* **124**, 030501 (2020).
- [110] J. J. Meyer, S. Khatri, D. Stilck França, J. Eisert, and P. Faist, Quantum metrology in the finite-sample regime, *PRX Quantum* **6**, 030336 (2025).
- [111] E. W. Weisstein, Chi-squared distribution, <https://mathworld.wolfram.com> (2002).

Appendix A: Related works on measurements for multi-parameter metrology

Here we present a detailed comparison of some traditional measurement protocols and our 3-design measurement protocol, as an extension of [Table I](#) in the main text. (Note that we have listed only the most relevant protocols below; there are other useful measurements not included here.)

Measurements	Family of States	Cost Matrix (Y/N)	Collective (Y/N)	Computational Complexity for Identifying POVMs	Implementation Complexity
3-design	Pure, Approximately low-rank, Full-parameter mixed states (Table II)	N	N	None	Efficient in multi-qubit systems
HCRB [26 , 39–41]	Mixed states	Y	Y (Infinite copies)	Unknown	Almost infeasible
HCRB [31]	Pure states	Y	N	Poly(d), Semidefinite programming [61]	Unknown
Direct optimization [32]	Mixed states	Y	N	NP-hard, Conic programming [65]	Unknown
Nagaoka–Hayashi [32 , 33]	Qubit states, Other examples	Y	N	-	-
Gill–Massar [30 , Sec.VII]	Qubit states	N	N	-	-
Fisher-symmetric [47 , 49]	Pure states	N	N	\leq Poly(d)	Unknown
Haar [101]	Pure states	N	N	None	Almost infeasible
2-design [48]	Pure states	N	Y (Two copies)	None	Platform-dependent
2-design [48]	Full-parameter maximally mixed states	N	N	None	Efficient in multi-qubit systems

Table III. Comparison of different types of measurements for multi-parameter metrology. We compare them using multiple features including: (1) Families of parameterized states, for which the measurements are optimal (under certain metric). This describes the generality of the measurement protocol. (2) Dependence on cost matrices, which determines whether the WMSE is minimized based on a specific cost matrix or the CFIM $I(M)$ is optimized to be as close to J as possible. In the former case, the cost matrix must be specified before the measurement is selected and there is no guarantee of optimality under other cost matrices. (3) Whether collective measurements are required, i.e., whether the POVM needs to be performed on more than one copies of the quantum state. Collective measurements are usually considered to be difficult to implement than individual measurements. (4) Computational complexity to solve for optimal POVMs. Note that when measurements are state-independent, i.e., universally optimal, e.g., 3-design, Haar and 2-design, there is no need to solve for them and thus we mark the computational complexity here as “None”. The computational complexity required for identifying the optimal POVM for the mixed-state HCRB is expected to be superpolynomial in d . Even though the value of HCRB is computable in Poly(d) [[61](#)], the known optimal POVM needs to be performed on at least Poly(d) copies of quantum states and requires a classical computer of size at least superpolynomial in d to store [[39](#)] (For the Nagaoka–Hayashi and Gill–Massar bounds, only special types of states were known to have optimal measurements in explicit forms; and thus we do not specify the computational or implementation complexity in this table.) (5) Implementation complexity. The complexity to implement POVMs was rarely investigated in literature of HCRB (and its variants). The complexity to implement an arbitrary unitary operation is a d -dimensional system is $\Omega(d)$ [[98](#)]. Thus, the implementation complexity of POVMs will be considered exponential in qubit number, unless with known simplifications. The implementation of two-copy measurements, though may be feasible in some physical platforms (e.g., [[100](#)]), can suffer from issues in synchronization, cross talks, and decoherence in general and thus is platform-dependent.

Appendix B: Justification of the definition of weak near-optimality

In this appendix, we justify the definition of weak near-optimality ([Definition 2](#)).

First, we note that it is impossible to define weak near-optimality without choosing a specific cost matrix as in Eq. (27). If for some measurement M , there exists a constant $c > 0$ such that for *all* cost matrices $W \succeq 0$,

$$\forall \tilde{M}, \quad \text{Tr}(W \cdot I(M)^{-1}) \leq c \text{Tr}(W \cdot I(\tilde{M})^{-1}), \quad (\text{B1})$$

then

$$\exists c > 0, \forall \tilde{M}, \quad I(M) \succeq cI(\tilde{M}), \quad (\text{B2})$$

It then implies

$$I(M) \succeq cJ, \quad (\text{B3})$$

because if Eq. (B3) is violated, there must be some specific parameter, which may be a linear combination of $\{\theta_i\}_i$, such that its CFI is smaller than c times its QFI, violating the saturability of single-parameter CR bound (Eq. (16)). Therefore, M must be near-optimal.

Second, we prove some meaningful properties of the weak near-optimality conditions.

(1) It is independent of parameterization. To be specific, when we view ρ_θ as ρ_φ which is a function of φ where φ is a new set of parameters defined by $\varphi_i = \sum_j A_{ij}\theta_j$ for some invertible matrix A . We have $A^T I(M)|_{\rho_\varphi} A = I(M)|_{\rho_\theta}$ and $A^T J|_{\rho_\varphi} A = J|_{\rho_\theta}$ and $\text{Tr}(J|_{\rho_\varphi} \cdot I(M)^{-1}|_{\rho_\varphi}) = \text{Tr}(J|_{\rho_\theta} \cdot I(M)^{-1}|_{\rho_\theta})$, showing Eq. (27)'s invariance under reparameterization. Eq. (28) is also invariant under reparameterization, noting that $\text{Tr}(J^{-1}|_{\rho_\varphi} \cdot I(M)|_{\rho_\varphi}) = \text{Tr}(J^{-1}|_{\rho_\theta} \cdot I(M)|_{\rho_\theta})$.

(2) It is a necessary condition of near-optimality. If a measurement is near-optimal, then $I(M) \succeq cJ \succeq cI(\tilde{M})$ for some c any \tilde{M} and Eq. (27) is satisfied. Eq. (28) also holds because

$$I(M) \succeq c \frac{\text{Tr}(J^{-1}J)}{\text{Tr}(J^{-1}J)} J \succeq c \frac{\text{Tr}(J^{-1}I(M))}{m} J. \quad (\text{B4})$$

(3) It is a proper generalization of the near-optimality condition, i.e., *for any state where near-optimal measurements exist, weakly near-optimal measurements are also near-optimal*. Suppose \tilde{M} is near-optimal and $I(\tilde{M}) \succeq cJ$, and M is weakly near-optimal. Then $\text{Tr}(JI(M)^{-1}) \leq c_1 \text{Tr}(JI(\tilde{M})^{-1}) \leq \frac{c_1}{c} m$ from Eq. (27), and from Eq. (28),

$$I(M) \succeq c_2 \frac{\text{Tr}(J^{-1}I(M))}{m} J \succeq c_2 \frac{m}{m \text{Tr}(JI(M)^{-1})} J \succeq \frac{cc_2}{c_1} J. \quad (\text{B5})$$

Therefore, M must be near-optimal.

(4) In single-parameter estimation (i.e., $m = 1$), the weak near-optimality condition and the near-optimality condition are equivalent. In particular, when $m = 1$, Eq. (27) is equivalent to the near-optimality condition and Eq. (28) is trivially true. Note that Sec. VII B contains an example of single-parameter estimation on mixed states where randomized measurements are proven to be not near-optimal, and they are also not weakly near-optimal according to this property.

(5) It is a proper generalization of the Fisher-symmetry condition. The Fisher-symmetry condition describes the optimality of measurements for local state tomography and is defined only for full-parameter quantum states (i.e., when m is maximal). Specifically, a POVM is called Fisher-symmetric [47, 48] if $I(M) \propto J$ and the GM bound is saturated at $\text{Tr}(J^{-1}I(M)) = d - 1$. Or equivalently, a POVM is Fisher-symmetric if and only if

$$I(M) = \frac{d-1}{m} J, \quad (\text{B6})$$

which makes sure M provides uniform and maximal information on all parameters.

Below we show the Fisher-symmetry condition is *almost*⁴ equivalent to the weak near-optimality condition.

We first show *any Fisher-symmetric measurement is weakly near-optimal*. For full-parameter pure states, a measurement is Fisher-symmetric if and only if $I(M) = \frac{1}{2}J$ [47] and it is clearly near-optimal and thus weakly near-optimal.

⁴ Note that in contrast to the Fisher-symmetry condition which defines the optimality of measurement in an exact fashion, the weak near-optimality is defined in an approximate fashion (i.e., we tolerate any constant-factor suboptimality). Therefore, we cannot hope for an exact equivalence between the Fisher-symmetry condition and the weak near-optimality condition. If we fix $c_1 = c_2 = 1$ in the definition of weak near-optimality, the equivalence will be exact.

For full-parameter full-rank mixed states, a measurement is Fisher-symmetric if and only if $I(M) = \frac{1}{d+1}J$. It implies that $\text{Tr}(JI(\tilde{M})^{-1})$ is minimized at $m^2/(d-1) = m(d+1)$ when $\tilde{M} = M$ from Cauchy-Schwarz (Eq. (23)). The first equality is satisfied because $I(M) \propto J$ and the second equality holds because $\text{Tr}(J^{-1}I(M)) = d-1$ and $m = d^2 - 1$. Thus, $\text{Tr}(JI(M)^{-1}) \leq \text{Tr}(JI(\tilde{M})^{-1})$ for any POVM \tilde{M} . Furthermore, $I(M) = \frac{\text{Tr}(J^{-1}I(M))}{m}J$ because $I(M) \propto J$. Thus M is weakly near-optimal.

Next, we show *whenever “nearly” Fisher-symmetric measurements exist, weakly near-optimal measurements are also nearly Fisher-symmetric*. Here a measurement is called nearly Fisher-symmetric if

$$I(M) \succeq c \frac{d-1}{m} J \quad (\text{B7})$$

for some positive constant c (as a relaxation of the exact case $I(M) = \frac{d-1}{m}J$). For full-parameter full-rank mixed states, $m = d^2 - 1$. Let \tilde{M} be a nearly Fisher-symmetric measurement, Eq. (27) implies $\text{Tr}(JI(M)^{-1}) \leq c_1 \text{Tr}(JI(\tilde{M})^{-1}) \leq \frac{c_1}{c} (d+1)^2 (d-1)$. Then

$$\text{Tr}(I(M)J^{-1}) \geq \frac{m^2}{\text{Tr}(JI(M)^{-1})} \geq \frac{c(d^2-1)^2}{c_1(d+1)(d^2-1)} = \frac{c(d-1)}{c_1}, \quad (\text{B8})$$

and then from Eq. (28),

$$I(M) \succeq c_2 \frac{\text{Tr}(I(M)J^{-1})}{m} J \succeq c_2 \frac{c(d-1)}{c_1(d^2-1)} J = \frac{cc_2(d-1)}{c_1 m} J. \quad (\text{B9})$$

The same analysis also works for full-parameter pure states.

Finally, we remark that the discussion above also shows if we require $c_1 = c_2 = 1$ in the definition of weak-optimality (Definition 2), the Fisher-symmetry condition would be exactly equivalent to the weak near-optimality condition, whenever Fisher-symmetric measurements exist.

Appendix C: Proof of Eq. (66)

Here we provide a proof of Eq. (66) that appear in Sec. V.

Let \mathbf{v} be an arbitrary vector in \mathbb{R}^m , we have

$$\mathbf{v}^T \tilde{K} \mathbf{v} = \sum_{jk: \lambda_j \text{ or } \lambda_k \geq \mu} \left(\frac{2 \langle \psi_j | \sum_i v_i \partial_i \rho | \psi_k \rangle + \sum_i v_i \partial_i p \delta_{jk}}{\lambda_j + \lambda_k} + \frac{\sum_{i'} v_{i'} \partial_{i'} p \delta_{kj}}{1-p} \right) \left(\frac{2 \langle \psi_k | \sum_{i'} v_{i'} \partial_{i'} \rho | \psi_j \rangle + \sum_{i'} v_{i'} \partial_{i'} p \delta_{kj}}{\lambda_j + \lambda_k} + \frac{\sum_{i'} v_{i'} \partial_{i'} p \delta_{kj}}{1-p} \right) \quad (\text{C1})$$

$$= \sum_{jk: \lambda_j \text{ or } \lambda_k \geq \mu} 4 \frac{|\langle \psi_j | \sum_i v_i \partial_i \rho | \psi_k \rangle|^2}{(\lambda_j + \lambda_k)^2} + \frac{\sum_i v_i \partial_i p}{1-p} \sum_{j: \lambda_j \geq \mu} 2 \frac{\langle \psi_j | \sum_i v_i \partial_i \rho | \psi_j \rangle}{\lambda_j} + d_{\Pi} \left(\frac{\sum_i v_i \partial_i p}{1-p} \right)^2 \quad (\text{C2})$$

$$= \sum_{jk: \lambda_j \text{ or } \lambda_k \geq \mu} 4 \frac{|\langle \psi_j | \sum_i v_i \partial_i \rho | \psi_k \rangle|^2}{(\lambda_j + \lambda_k)^2} + 2 \frac{\sum_i v_i \partial_i p}{1-p} \left(\sum_{i,j: \lambda_j \geq \mu} v_i \frac{\partial_i \lambda_j}{\lambda_j} \right) + d_{\Pi} \left(\frac{\sum_i v_i \partial_i p}{1-p} \right)^2 \quad (\text{C3})$$

$$\leq \sum_{jk: \lambda_j \text{ or } \lambda_k \geq \mu} 4 \frac{|\langle \psi_j | \sum_i v_i \partial_i \rho | \psi_k \rangle|^2}{(\lambda_j + \lambda_k)^2} + \left(\sum_{i,j: \lambda_j \geq \mu} v_i \frac{\partial_i \lambda_j}{\lambda_j} \right)^2 + (d_{\Pi} + 1) \left(\frac{\sum_i v_i \partial_i p}{1-p} \right)^2 \quad (\text{C4})$$

$$\leq \sum_{jk: \lambda_j \text{ or } \lambda_k \geq \mu} 4 \frac{|\langle \psi_j | \sum_i v_i \partial_i \rho | \psi_k \rangle|^2}{(\lambda_j + \lambda_k)^2} + \sum_{jk: \lambda_{j,k} \geq \mu} \frac{(\sum_i v_i \partial_i \lambda_j)^2}{\lambda_j \lambda_k} + (d_{\Pi} + 1) \left(\frac{\sum_i v_i \partial_i p}{1-p} \right)^2 \quad (\text{C5})$$

$$\leq \frac{1}{\mu} \sum_{jk: \lambda_j \text{ or } \lambda_k \geq \mu} 4 \frac{|\langle \psi_j | \sum_i v_i \partial_i \rho | \psi_k \rangle|^2}{\lambda_j + \lambda_k} + \frac{1}{\mu} \sum_{jk: \lambda_{j,k} \geq \mu} \frac{(\sum_i v_i \partial_i \lambda_j)^2}{\lambda_j} + (d_{\Pi} + 1) \left(\frac{\sum_i v_i \partial_i p}{1-p} \right)^2 \quad (\text{C6})$$

$$\leq \frac{2}{\mu} \mathbf{v}^T J \mathbf{v} + \frac{1}{\mu} \mathbf{v}^T J \mathbf{v} + \frac{p(d_{\Pi} + 1)}{1-p} \mathbf{v}^T J^p \mathbf{v} \quad (\text{C7})$$

$$\leq \frac{3}{\mu} \mathbf{v}^T J \mathbf{v} + \frac{d_{\Pi} + 1}{d_{\Pi} \mu} \mathbf{v}^T J^p \mathbf{v} \leq \frac{5}{\mu} \mathbf{v}^T J \mathbf{v}. \quad (\text{C8})$$

where $d_\Pi = \text{Tr}(\Pi)$ is the dimension of the subspace Π . In the third and seventh line we use $\langle \psi_j | \partial_i \rho | \psi_j \rangle = \partial_i \lambda_j + \lambda_j (\partial_i \langle \psi_j | \psi_j \rangle) = \partial_i \lambda_j$, in the fourth and fifth line we use $2ab \leq a^2 + b^2$ for any $a, b \in \mathbb{R}$ and in the eighth line we use $d_\Pi \mu \leq 1 - p$, $(d_\Pi + 1)/d_\Pi \leq 2$, and $J^p \preceq J$. Eq. (66) is then proved.

Appendix D: Generalization of the GM bound

Here we review the proof of the GM bound [30] and extend it to all cases discussed in Theorem 4.

To prove the GM bound (Eq. (22)), it is first important to notice that the GM quantity $\text{Tr}(J^{-1}I(M))$ is independent of reparameterization. That means, it is sufficient to prove the GM bound using one specific parameterization of our choice. Let $\rho_\theta = \sum_{k=1}^r \lambda_k |\psi_k\rangle \langle \psi_k|$ where $\lambda_k > 0$ for $k \in \{1, 2, \dots, r\} =: [r]$. $\lambda_\ell = 0$ for $\ell \in \{r+1, r+2, \dots, d\}$. (Note that the original proof [30] contains the cases of $r = 1, d$ and here we generalize the discussion to arbitrary r). We can, without loss of generality, assume the number of unknown parameters is maximal, because increase the number of parameters can only increase the GM quantity $\text{Tr}(J^{-1}I(M))$ [30]. We choose the following complete set of traceless Hermitian operator basis,

$$\rho_{,k\ell+} = |\psi_k\rangle \langle \psi_\ell| + |\psi_\ell\rangle \langle \psi_k|, \quad \rho_{,k\ell-} = i|\psi_k\rangle \langle \psi_\ell| - i|\psi_\ell\rangle \langle \psi_k|, \quad \forall k < \ell, k \in [r], \ell \in [d], \quad (\text{D1})$$

$$\rho_{,b} = \sum_{k=1}^r c_{bk} |\psi_k\rangle \langle \psi_k|, \quad \forall b = 1, \dots, r-1, \quad (\text{D2})$$

where

$$\sum_{k=1}^r c_{bk} = 0, \quad \sum_{k=1}^r \frac{1}{\lambda_k} c_{b'k} c_{bk} = \delta_{b'b}, \quad \forall b = 1, \dots, r-1. \quad (\text{D3})$$

Further let $c_{rk} = \lambda_k$ for all $k = 1, \dots, r$. We have $CA^{-1}C^T = \mathbb{1}$ from above, where C is a $r \times r$ real-valued matrix whose entries are given by c_{bk} for $b, k \in [r]$ and A^{-1} is a diagonal matrix whose diagonal entries are λ_k^{-1} . It then implies $\Lambda^{-1/2}C^TCA^{-1/2} = \mathbb{1}$, i.e.,

$$\sum_{b=1}^r \frac{c_{bk}c_{bk'}}{\sqrt{\lambda_k\lambda_{k'}}} = \sqrt{\lambda_k\lambda_{k'}} + \sum_{b=1}^{r-1} \frac{c_{bk}c_{bk'}}{\sqrt{\lambda_k\lambda_{k'}}} = \delta_{kk'}. \quad (\text{D4})$$

Consider a parameterization of ρ_θ such that $\partial_i \rho_\theta = \rho_{,i}$. The QFIM is

$$J_{k\ell\pm, k'\ell'\pm'} = \frac{4}{\lambda_k + \lambda_\ell} \delta_{kk'} \delta_{\ell\ell'} \delta_{\pm\pm'}, \quad J_{k\ell\pm, b} = 0, \quad J_{b, b'} = \delta_{bb'}, \quad (\text{D5})$$

where $(k, \ell) \in [r] \times [d]$ and $b \in [r-1]$. Since the CFIM $I(M)$ cannot decrease if we replace any measurement operator M_1 with its refinement $\{M_2, M_3\}$ where $M_1 = M_2 + M_3$, it is sufficient to consider a POVM with rank-one operators ($|\phi_x\rangle$ is unnormalized),

$$M_x = |\phi_x\rangle \langle \phi_x|, \quad |\phi_x\rangle = \sum_{k=1}^d a_{xk} |\psi_k\rangle. \quad (\text{D6})$$

Then we have

$$\text{Tr}(J^{-1}I(M)) = \sum_x \frac{1}{\langle \phi_x | \rho_\theta | \phi_x \rangle} \left(\sum_{\substack{k < \ell \\ k, \ell \in [r] \times [d]}} \sum_{\pm} \frac{\lambda_k + \lambda_\ell}{4} \langle \phi_x | \rho_{,k\ell\pm} | \phi_x \rangle^2 + \sum_{b=1}^{r-1} \langle \phi_x | \rho_{,b} | \phi_x \rangle^2 \right) \quad (\text{D7})$$

$$= \sum_x \frac{1}{\langle \phi_x | \rho_\theta | \phi_x \rangle} \left(\sum_{\substack{k < \ell \\ k, \ell \in [r] \times [d]}} (\lambda_k + \lambda_\ell) |a_{xk}|^2 |a_{x\ell}|^2 + \sum_{b=1}^{r-1} \left(\sum_k |a_{xk}|^2 c_{bk} \right)^2 \right) \quad (\text{D8})$$

$$= \sum_x \frac{1}{\langle \phi_x | \rho_\theta | \phi_x \rangle} \left(\sum_{k, \ell=1}^r |a_{xk}|^2 |a_{x\ell}|^2 \lambda_k (1 - \lambda_\ell) + \sum_{k=1}^r \sum_{\ell=r+1}^d |a_{xk}|^2 |a_{x\ell}|^2 (\lambda_k + \lambda_\ell) \right) \quad (\text{D9})$$

$$= \sum_x \left(\sum_{\ell=1}^d |a_{x\ell}|^2 (1 - \lambda_\ell) \right) = \sum_x \text{Tr}((\mathbb{1} - \rho_\theta)M_x) = d - 1, \quad (\text{D10})$$

where in the first line we simply plug in the definition of $I(M)$ where $I(M)_{ij} = \sum_x \frac{\langle \phi_x | \partial_i \rho_\theta | \phi_x \rangle \langle \phi_x | \partial_j \rho_\theta | \phi_x \rangle}{\langle \phi_x | \rho_\theta | \phi_x \rangle}$, in the third line we use Eq. (D4) to eliminate c_{bk} , and in the last line we use $\lambda_\ell = 0$ when $\ell \geq r+1$ and $\langle \phi_x | \rho_\theta | \phi_x \rangle = \sum_{k=1}^r \lambda_k |a_{xk}|^2$. This proves Eq. (22) in the main text.

Consider the second case in Theorem 4, where $\partial_i \rho_\theta$ are restricted to the support of ρ_θ . In this case, we exclude $\rho_{,k\ell\pm}$ from the derivative operators where $k \in [r]$ and $\ell \in [d] \setminus [r]$. We have

$$\text{Tr}(J^{-1}I(M)) = \sum_x \frac{1}{\langle \phi_x | \rho_\theta | \phi_x \rangle} \left(\sum_{\substack{k < \ell \\ k, \ell \in [r] \times [r]}} \sum_{\pm} \frac{\lambda_k + \lambda_\ell}{4} \langle \phi_x | \rho_{,k\ell\pm} | \phi_x \rangle^2 + \sum_{b=1}^{r-1} \langle \phi_x | \rho_{,b} | \phi_x \rangle^2 \right) \quad (\text{D11})$$

$$= \sum_x \frac{1}{\langle \phi_x | \rho_\theta | \phi_x \rangle} \left(\sum_{\substack{k < \ell \\ k, \ell \in [r] \times [r]}} (\lambda_k + \lambda_\ell) |a_{xk}|^2 |a_{x\ell}|^2 + \sum_{b=1}^{r-1} \left(\sum_k |a_{xk}|^2 c_{bk} \right)^2 \right) \quad (\text{D12})$$

$$= \sum_x \frac{1}{\langle \phi_x | \rho_\theta | \phi_x \rangle} \left(\sum_{k, \ell=1}^r |a_{xk}|^2 |a_{x\ell}|^2 \lambda_k (1 - \lambda_\ell) \right) \quad (\text{D13})$$

$$= \sum_x \left(\sum_{\ell=1}^r |a_{x\ell}|^2 (1 - \lambda_\ell) \right) = \sum_x \text{Tr}(\Pi(\mathbb{1} - \rho_\theta)\Pi M_x) = r - 1, \quad (\text{D14})$$

where Π is the projector onto the support of ρ_θ . This proves Eq. (75) in the main text.

Consider the third case in Theorem 4, where $\partial_i \rho_\theta$ are restricted outside the support of ρ_θ . In this case, we exclude $\rho_{,k\ell\pm}$ and $\rho_{,b}$ from the derivative operators where $k, \ell, b \in [r]$. We have

$$\text{Tr}(J^{-1}I(M)) = \sum_x \frac{1}{\langle \phi_x | \rho_\theta | \phi_x \rangle} \left(\sum_{k, \ell \in [r] \times ([d] \setminus [r])} \sum_{\pm} \frac{\lambda_k + \lambda_\ell}{4} \langle \phi_x | \rho_{,k\ell\pm} | \phi_x \rangle^2 \right) \quad (\text{D15})$$

$$= \sum_x \frac{1}{\langle \phi_x | \rho_\theta | \phi_x \rangle} \left(\sum_{k=1}^r \sum_{\ell=r+1}^d |a_{xk}|^2 |a_{x\ell}|^2 (\lambda_k + \lambda_\ell) \right) \quad (\text{D16})$$

$$= \sum_x \left(\sum_{\ell=r+1}^d |a_{x\ell}|^2 \right) = \sum_x \text{Tr}((\mathbb{1} - \Pi)M_x) = d - r. \quad (\text{D17})$$

This proves Eq. (76) in the main text.

Appendix E: Concentration inequality for complex projective Haar measure

In this section, we prove a concentration inequality of the (complex projective) Haar measure, which is used to derive Eq. (93).

Lemma S1. *Let $|\phi\rangle$ be a fixed d -dimensional state. Let μ_s be the (complex projective) Haar measure. For any $x \in [0, 1]$,*

$$\Pr_{s \sim \mu_s} [|\langle s | \phi \rangle|^2 \leq x] \leq (d - 1)x. \quad (\text{E1})$$

Proof. Let $\{|0\rangle, |1\rangle, \dots, |d-1\rangle\}$ be an orthonormal basis for the d -dimensional Hilbert space. By the unitary invariance of (complex projective) Haar measure, we can take $|\phi\rangle = |0\rangle$. The state $|s\rangle$ sampled from the (complex projective) Haar measure can be expressed by (see e.g. [68, Sec. 7.2]):

$$|s\rangle := \frac{|\tilde{s}\rangle}{\sqrt{\langle \tilde{s} | \tilde{s} \rangle}}, \quad |\tilde{s}\rangle := \sum_{k=0}^{d-1} (X_k + iY_k) |k\rangle. \quad (\text{E2})$$

where X_k, Y_k are independent standard normal random variables. Thus,

$$|\langle s|0\rangle|^2 = \frac{|\langle \tilde{s}|0\rangle|^2}{\langle \tilde{s}|\tilde{s}\rangle} = \frac{X_0^2 + Y_0^2}{\sum_{k=0}^{d-1} (X_k^2 + Y_k^2)}. \quad (\text{E3})$$

The probability we want to calculate can be computed as

$$\begin{aligned} \Pr[|\langle s|0\rangle|^2 \leq x] &= \Pr\left[\sum_{k=1}^{d-1} (X_k^2 + Y_k^2) \geq (x^{-1} - 1)(X_0^2 + Y_0^2)\right] \\ &= \int_0^{+\infty} d\alpha \frac{1}{2} e^{-\alpha/2} \frac{\Gamma(d-1, \frac{1}{2}(x^{-1} - 1)\alpha)}{\Gamma(d-1)} \\ &= 1 - (1-x)^{d-1} \\ &\leq (d-1)x. \end{aligned} \quad (\text{E4})$$

Here we use the fact that $X_0^2 + Y_0^2$ and $\sum_{k=1}^{d-1} (X_k^2 + Y_k^2)$ are independent χ^2 distributions with 2 and $2(d-1)$ degrees of freedom, respectively [111]. The probability density function and the (upper) cumulative distribution function of χ^2 distributions with k degrees of freedom are given by,

$$p(\alpha) = \frac{\alpha^{\frac{k}{2}-1} e^{-\alpha}}{2^{k/2} \Gamma(k/2)}, \quad \int_{\alpha}^{+\infty} d\beta p(\beta) = \frac{\Gamma(k/2, \alpha/2)}{\Gamma(k/2)}, \quad (\text{E5})$$

where $\Gamma(\star, \star)$ is the upper incomplete Gamma function and $\Gamma(\star)$ is the Gamma function. This completes the proof. \square

Appendix F: Proof of Eq. (126)

Here we prove Eq. (126) in the main text, i.e.,

$$J(\psi^{\text{ME}})_{ij} = J[(\mathcal{E}_\theta \otimes \mathbb{1})(\psi^{\text{ME}})]_{ij} = 2\delta_{ij} \sum_{k:q_k+q_{k+i}>0} \frac{|q_{k+i} - q_k|^2}{q_k + q_{k+i}}. \quad (\text{F1})$$

First, we note that the eigenstates of $\rho_\theta := (\mathcal{E}_\theta \otimes \mathbb{1})(\psi^{\text{ME}})$ are

$$|\psi_k\rangle := P_k \otimes \mathbb{1} |\psi^{\text{ME}}\rangle, \quad (\text{F2})$$

with eigenvalues q_k for $k = 0, \dots, d^2 - 1$. Then

$$J(\psi^{\text{ME}})_{ij} = 2 \sum_{k\ell:q_k+q_\ell>0} \frac{\text{Re}[\langle \psi_k | \partial_i \rho_\theta | \psi_\ell \rangle \langle \psi_\ell | \partial_j \rho_\theta | \psi_k \rangle]}{q_k + q_\ell}. \quad (\text{F3})$$

Note that

$$\begin{aligned} \langle \psi_k | \partial_i \rho_\theta | \psi_\ell \rangle &= -\langle \psi_k | \left(\sum_{k'} i q_{k'} P_{k'} P_i | \psi_0 \rangle \langle \psi_0 | P_{k'} - i q_{k'} P_{k'} | \psi_0 \rangle \langle \psi_0 | P_i P_{k'} \right) | \psi_\ell \rangle \\ &= \sum_{k'} -i q_{k'} \eta_{k'i} \delta_{k,k'+i} \delta_{k'\ell} + i q_{k'} \eta_{k'i}^* \delta_{kk'} \delta_{i+k',\ell} = -\delta_{k+i,\ell} i q_\ell \eta_{\ell i} + \delta_{k+i,\ell} i q_k \eta_{ki}^*. \end{aligned} \quad (\text{F4})$$

Here η_{ij} is defined through $P_{i+j} = \eta_{ij} P_i P_j$ and $\eta_{k,i} \in \{\pm 1, \pm i\}$ makes sure $P_{k+i} \in \{\mathbb{1}, \sigma_x, \sigma_y, \sigma_z\}^{\otimes n}$. $\eta_{ij} = \pm 1$ when $[P_i, P_j] = 0$ and $\eta_{ij} = \pm i$ when $[P_i, P_j] \neq 0$. We also use $\langle \psi_0 | P_i P_j | \psi_0 \rangle = \frac{1}{d} \text{Tr}(P_i P_j) = \delta_{ij}$ above. Then

$$\text{Re}[\langle \psi_k | \partial_i \rho_\theta | \psi_\ell \rangle \langle \psi_\ell | \partial_j \rho_\theta | \psi_k \rangle] = \delta_{ij} \delta_{k+i,\ell} |q_\ell \eta_{\ell i} - q_k \eta_{ki}^*|^2. \quad (\text{F5})$$

We have

$$J(\psi^{\text{ME}})_{ij} = 2\delta_{ij} \sum_{k\ell:q_k+q_\ell>0} \frac{\delta_{k+i,\ell} |q_\ell \eta_{\ell i} - q_k \eta_{ki}^*|^2}{q_k + q_\ell} = 2\delta_{ij} \sum_{k:q_k+q_{k+i}>0} \frac{|q_{k+i} \eta_{k+i,i} - q_k \eta_{ki}^*|^2}{q_k + q_{k+i}}. \quad (\text{F6})$$

Finally, note that

$$P_{k+i}P_k = (P_{k+i}P_i)(P_iP_k) = (\eta_{k+i,i}P_k)(\eta_{ik}P_{k+i}) = \eta_{k+i,i}\eta_{ik}P_kP_{k+i}. \quad (\text{F7})$$

When $[P_i, P_k] = 0$, we have $[P_{k+i}, P_k] = 0$ and $\eta_{ik} = \pm 1 = -\eta_{k+i,i}$. When $[P_i, P_k] \neq 0$, we have $[P_{k+i}, P_k] \neq 0$ and $\eta_{ik} = \pm i = \eta_{k+i,i}$. Also note that $\eta_{ik} = \eta_{ki}^*$. We have

$$J(\psi^{\text{ME}})_{ij} = 2\delta_{ij} \sum_{k:q_k+q_{k+i}>0} \frac{|q_{k+i} - q_k|^2}{q_k + q_{k+i}}. \quad (\text{F8})$$

Appendix G: Proofs of Eq. (135) and Eq. (138), Computing deviation observables

Here we first prove Eq. (135) in the main text, i.e.,

$$J(\psi^{\text{C},(0)}) - \tilde{q}J^\perp(\psi^{\text{C},(0)}) \succeq \frac{(1-2q)^2 - q}{(1-2q)^2} J(\psi^{\text{C},(0)}) \quad (\text{G1})$$

We first compute $J(\psi^{\text{C},(0)})$, given by

$$\begin{aligned} J(\psi^{\text{C},(0)})_{jj'} &= J[\mathcal{E}_\theta(\psi^{\text{C},(0)})] = J\left[\sum_{k=0}^{d^2-1} q_k P_k U_\theta \psi^{\text{C},(0)} U_\theta^\dagger P_k\right]_{jj'} \\ &= \sum_{\substack{x,y \in \{0,1\}^n \\ \tilde{q}_x + \tilde{q}_y > 0}} \frac{2\text{Re}[\langle x | \partial_j \rho_\theta | y \rangle \langle y | \partial_{j'} \rho_\theta | x \rangle]}{\tilde{q}_x + \tilde{q}_y}, \end{aligned} \quad (\text{G2})$$

where $\rho_\theta := \mathcal{E}_\theta(\psi^{\text{C},(0)})$ and $|x\rangle = |x_1, x_2, \dots, x_n\rangle$ are the computational basis, as eigenstates of ρ_θ at $\theta = 0$. $\tilde{q}_x := \sum_{k:\tilde{k}=x} q_k$ are the corresponding eigenvalues. Note that

$$\langle x | \partial_j \rho_\theta | y \rangle = \sum_k q_k (-i \langle x | P_k P_j | 0^{\otimes n} \rangle \langle 0^{\otimes n} | P_k | y \rangle + i \langle x | P_k | 0^{\otimes n} \rangle \langle 0^{\otimes n} | P_j P_k | y \rangle) \quad (\text{G3})$$

is non-zero only when $\tilde{j} = \tilde{x} + \tilde{y}$. This implies $J(\psi^{\text{C},(0)})$ must be block-diagonal in the sense that $J(\psi^{\text{C},(0)})_{jj'} = J(\psi^{\text{C},(0)})_{jj'} \delta_{\tilde{j}\tilde{j}'}$. Below we will use a matrix B to lower bound $J(\psi^{\text{C},(0)})$ where $J(\psi^{\text{C},(0)}) \succeq B$, and

$$B_{jj'} := \delta_{\tilde{j}\tilde{j}'} \left(\frac{2\text{Re}[\langle 0^{\otimes n} | \partial_j \rho_\theta | \tilde{j} \rangle \langle \tilde{j} | \partial_{j'} \rho_\theta | 0^{\otimes n} \rangle]}{\tilde{q}_0 + \tilde{q}_{\tilde{j}}} + \frac{2\text{Re}[\langle \tilde{j} | \partial_j \rho_\theta | 0^{\otimes n} \rangle \langle 0^{\otimes n} | \partial_{j'} \rho_\theta | \tilde{j} \rangle]}{\tilde{q}_0 + \tilde{q}_{\tilde{j}}} \right), \quad (\text{G4})$$

where we specifically pick out two terms $(x, y) = (0, \tilde{j})$ and $(x, y) = (\tilde{j}, 0)$ from $J(\psi^{\text{C},(0)})$. On the other hand, we have

$$J^\perp(\psi^{\text{C},(0)}) \preceq J[\psi_\theta^{\text{C},(0)}], \quad J[\psi_\theta^{\text{C},(0)}]_{jj'} = 4(\langle 0^{\otimes n} | \{P_j, P_{j'}\} | 0^{\otimes n} \rangle - \langle 0^{\otimes n} | P_j | 0^{\otimes n} \rangle \langle 0^{\otimes n} | P_{j'} | 0^{\otimes n} \rangle). \quad (\text{G5})$$

Our goal is then to show

$$B - \tilde{q}J[\psi_\theta^{\text{C},(0)}] \succeq \frac{(1-2q)^2 - q}{(1-2q)^2} B. \quad (\text{G6})$$

Both $B_{jj'}$ and $J[\psi_\theta^{\text{C},(0)}]_{jj'}$ are zero when $\tilde{j} \neq \tilde{j}'$. Therefore, it is sufficient to show Eq. (G6) for blocks of matrices with the same \tilde{j} , i.e.,

$$\mathbf{P}_{\tilde{j}} B \mathbf{P}_{\tilde{j}} - \tilde{q} \mathbf{P}_{\tilde{j}} J[\psi_\theta^{\text{C},(0)}] \mathbf{P}_{\tilde{j}} \succeq \frac{(1-2q)^2 - q}{(1-2q)^2} \mathbf{P}_{\tilde{j}} B \mathbf{P}_{\tilde{j}}. \quad (\text{G7})$$

for all $\tilde{j} \in \{0, 1\}^n$, where the projector $\mathbf{P}_{\tilde{j}} = \sum_{j': \tilde{j}' = \tilde{j}} |j'\rangle \langle j'|$. Note that when $\mathbf{P}_0 B \mathbf{P}_0 = \mathbf{P}_0 J[\psi_\theta^{\text{C},(0)}] \mathbf{P}_0 = 0$. Therefore, we assume $\tilde{j} \neq 0^n$, and prove Eq. (G7) below. We have

$$\langle 0^{\otimes n} | \partial_j \rho_\theta | \tilde{j} \rangle = \sum_{k, \tilde{k} = \tilde{j}} q_k (-i \langle 0^{\otimes n} | P_k P_j | 0^{\otimes n} \rangle \langle 0^{\otimes n} | P_k | \tilde{j} \rangle) + \sum_{k, \tilde{k} = 0} q_k (i \langle 0^{\otimes n} | P_k | 0^{\otimes n} \rangle \langle 0^{\otimes n} | P_j P_k | \tilde{j} \rangle)$$

$$\begin{aligned}
&= \sum_{k, \bar{k}=\tilde{j}} q_k (-i(-1)^{\nu_k} i^{\nu_j}) + \sum_{k, \bar{k}=0} q_k \left(i(-i)^{\nu_j} (-1)^{z_k \cdot \tilde{j}} \right) \\
&= q_0 i (-i)^{\nu_j} \left(1 + (-1)^{\nu_j+1} \sum_{k, \bar{k}=\tilde{j}} \frac{q_k}{q_0} (-1)^{\nu_k} + \sum_{k: k \neq 0, \bar{k}=0} \frac{q_k}{q_0} (-1)^{z_k \cdot \tilde{j}} \right) \\
&= q_0 i \langle 0^{\otimes n} | P_j | \tilde{j} \rangle \left(1 + (-1)^{\nu_j+1} \sum_{k, \bar{k}=\tilde{j}} \frac{q_k}{q_0} (-1)^{\nu_k} + \sum_{k: k \neq 0, \bar{k}=0} \frac{q_k}{q_0} (-1)^{z_k \cdot \tilde{j}} \right) \\
&=: q_0 i \langle 0^{\otimes n} | P_j | \tilde{j} \rangle \left(1 + (-1)^{\nu_j+1} g_1(\tilde{j}) + g_2(\tilde{j}) \right), \quad \text{where } i \langle 0^{\otimes n} | P_j | \tilde{j} \rangle = (-i)^{\nu_j}. \tag{G8}
\end{aligned}$$

Here ν_k denotes the number of Pauli Y's in P_k and z_k is an n -bit string whose elements are 1 at locations where P_k is Pauli Z and 0 otherwise. $|g_1(\tilde{j})| + |g_2(\tilde{j})| \leq \frac{q}{q_0}$. Then

$$B_{jj'} = \delta_{\tilde{j}\tilde{j}'} \frac{4q_0^2 \text{Re}[\langle 0^{\otimes n} | P_j | \tilde{j} \rangle \langle \tilde{j} | P_{j'} | 0^{\otimes n} \rangle] \left(1 + (-1)^{\nu_j+1} g_1(\tilde{j}) + g_2(\tilde{j}) \right) \left(1 + (-1)^{\nu_{j'}+1} g_1(\tilde{j}') + g_2(\tilde{j}') \right)}{\tilde{q}_0 + \tilde{q}_{\tilde{j}}} \tag{G9}$$

$$= J[\psi_\theta^{\text{C},(0)}]_{jj'} \delta_{\tilde{j}\tilde{j}'} \frac{q_0^2 \left(1 + (-1)^{\nu_j+1} g_1(\tilde{j}) + g_2(\tilde{j}) \right) \left(1 + (-1)^{\nu_{j'}+1} g_1(\tilde{j}') + g_2(\tilde{j}') \right)}{\tilde{q}_0 + \tilde{q}_{\tilde{j}}} \tag{G10}$$

When $\nu_j \neq \nu_{j'}$, the numbers of Pauli Y's in P_j and $P_{j'}$ do not have the same parity. Plus that $\tilde{j} = \tilde{j}'$, we have $\{P_j, P_{j'}\} = 0$ and $B_{jj'} = J[\psi_\theta^{\text{C},(0)}]_{jj'} = 0$. Therefore, we have

$$\begin{aligned}
B_{jj'} &= J[\psi_\theta^{\text{C},(0)}]_{jj'} \delta_{\tilde{j}\tilde{j}'} \delta_{\nu_j \nu_{j'}} \frac{q_0^2 \left(1 + (-1)^{\nu_j+1} g_1(\tilde{j}) + g_2(\tilde{j}) \right)^2}{\tilde{q}_0 + \tilde{q}_{\tilde{j}}} \\
&\geq J[\psi_\theta^{\text{C},(0)}]_{jj'} \delta_{\tilde{j}\tilde{j}'} \delta_{\nu_j \nu_{j'}} \frac{q_0^2 (1 - q/q_0)^2}{\tilde{q}_0 + \tilde{q}_{\tilde{j}}} \geq J[\psi_\theta^{\text{C},(0)}]_{jj'} \delta_{\tilde{j}\tilde{j}'} \delta_{\nu_j \nu_{j'}} (1 - 2q)^2. \tag{G11}
\end{aligned}$$

Therefore,

$$B \succeq J[\psi_\theta^{\text{C},(0)}] (1 - 2q)^2. \tag{G12}$$

This implies Eq. (G6), noting that $\tilde{q} \leq q$.

The above implies

$$J(\psi^{\text{C},(0)}) \succeq J[\psi_\theta^{\text{C},(0)}] (1 - 2q)^2, \tag{G13}$$

and this extends to all random stabilizer input states as explained in the main text. Then

$$\sum_i p^{\text{C},(i)} J(\psi^{\text{C},(i)}) \succeq \sum_i p^{\text{C},(i)} J[\psi_\theta^{\text{C},(i)}] (1 - 2q)^2 = \frac{4d}{d+1} (1 - 2q)^2 \mathbb{1}, \tag{G14}$$

which proves the last line in Eq. (138), where we use

$$\begin{aligned}
&\sum_i p^{\text{C},(i)} J[\psi_\theta^{\text{C},(i)}]_{jj'} = \\
&4 \sum_i p^{\text{C},(i)} \left(\langle 0^{\otimes n} | U^{(i)\dagger} \frac{1}{2} \{P_j, P_{j'}\} U^{(i)} | 0^{\otimes n} \rangle - \langle 0^{\otimes n} | U^{(i)\dagger} P_j U^{(i)} | 0^{\otimes n} \rangle \langle 0^{\otimes n} | U^{(i)\dagger} P_{j'} U^{(i)} | 0^{\otimes n} \rangle \right) = \frac{4d}{d+1} \delta_{jj'}. \tag{G15}
\end{aligned}$$

Here we use the 2-design property of the Clifford group. The same derivation has appeared in Eq. (118).

Finally, we explain how to compute the deviation observables. They are

$$X_j(\psi^{\text{C},(i)}; \theta) = \sum_k (\tilde{J}(\rho_{\text{RP}}^{\text{C}})^{-1})_{jk} \tilde{L}_k(\psi^{\text{C},(i)}). \tag{G16}$$

When $\psi^{C,(i)} = |0^{\otimes n}\rangle \langle 0^{\otimes n}|$,

$$\tilde{J}(\psi^{C,(0)})_{jj'} = B_{jj'} \quad (\text{details in Eq. (G4), Eq. (G8)}), \quad (\text{G17})$$

$$\tilde{L}_j(\psi^{C,(0)}) = \frac{2}{\tilde{q}_0 + \tilde{q}_j} (\langle 0^{\otimes n} | \partial_j \rho_\theta | \tilde{j} \rangle |0^{\otimes n}\rangle \langle \tilde{j}| + \langle \tilde{j} | \partial_j \rho_\theta |0^{\otimes n}\rangle | \tilde{j} \rangle \langle 0^{\otimes n} |) \quad (\text{details in Eq. (G8)}), \quad (\text{G18})$$

Generally, when $|\psi^{C,(i)}\rangle = U^{(i)\dagger} |0^{\otimes n}\rangle$, $\tilde{J}(\psi^{C,(i)})_{jj'}$ and $\tilde{L}_j(\psi^{C,(i)})$ can be calculated again using Eq. (G17) and Eq. (G18) with the following transformations:

- (1) \tilde{k} is an n -bit string where the l -th number \tilde{k}_l is equal to 1 if $U^{(i)\dagger} P_k U^{(i)}$ on the l -th qubit is σ_x or σ_y , and \tilde{k}_l is equal to 0 if $U^{(i)\dagger} P_k U^{(i)}$ on the l -th qubit is σ_z or $\mathbb{1}$ and $\tilde{q}_x = \sum_{k:\tilde{k}=\tilde{x}} q_k$ accordingly.
- (2) Similarly in Eq. (G8), ν_k denotes the number of Pauli Y's in $U^{(i)\dagger} P_k U^{(i)}$ and z_k is an n -bit string whose elements are 1 at locations where $U^{(i)\dagger} P_k U^{(i)}$ is Pauli Z and 0 otherwise.
- (3) $|0^{\otimes n}\rangle \langle \tilde{j}|$ and $|\tilde{j}\rangle \langle 0^{\otimes n}|$ in Eq. (G18) should be replaced with $U^{(i)} |0^{\otimes n}\rangle \langle \tilde{j}| U^{(i)\dagger}$ and $U^{(i)} |\tilde{j}\rangle \langle 0^{\otimes n}| U^{(i)\dagger}$.

Then deviation observables (Eq. (G16)) can be computed using Eq. (G17), Eq. (G18) and $\tilde{J}(\rho_{\text{RP}}^C) = \mathbb{E}_i[\tilde{J}(\psi^{C,(i)})]$.

Let us consider a special case of global depolarizing noise, where $q_0 = 1 - q$ and $q_k = \frac{q}{d^2 - 1}$ for all $k \neq 0$. When the input state is $|0^{\otimes n}\rangle$, we have for all $\tilde{j} \neq 0$,

$$g_1(\tilde{j}) = \sum_{k,\tilde{k}=\tilde{j}} \frac{q_k}{q_0} (-1)^{\nu_k} = 0, \quad g_2(\tilde{j}) = \sum_{k:k \neq 0, \tilde{k}=0} \frac{q_k}{q_0} (-1)^{z_k \cdot \tilde{j}} = -\frac{q}{(d^2 - 1)(1 - q)}, \quad (\text{G19})$$

$$\langle 0^{\otimes n} | \partial_j \rho_\theta | \tilde{j} \rangle = q_0 i (-i)^{\nu_j} (1 + (-1)^{\nu_j + 1} g_1(\tilde{j}) + g_2(\tilde{j})) = i (-i)^{\nu_j} \left(1 - q + \frac{q}{d^2 - 1}\right), \quad (\text{G20})$$

$$\tilde{J}(\psi^{C,(0)})_{jj'} = B_{jj'} = 4 \delta_{\tilde{j}\tilde{j}'} \delta_{\nu_j + \nu_{j'}, \text{ is even}} \frac{\left(1 - q + \frac{q}{d^2 - 1}\right)^2}{1 - q + \frac{q(2d-1)}{d^2 - 1}} (-1)^{\nu_j} (-1)^{\frac{\nu_j + \nu_{j'}}{2}}, \quad (\text{G21})$$

$$\Rightarrow \tilde{J}(\psi^{C,(0)})_{jj'} = \frac{\left(1 - q + \frac{q}{d^2 - 1}\right)^2}{1 - q + \frac{q(2d-1)}{d^2 - 1}} J[\psi_\theta^{C,(0)}]_{jj'}, \quad (\text{G22})$$

$$\tilde{L}_j(\psi^{C,(0)}) = \frac{1 - q + \frac{q}{d^2 - 1}}{1 - q + \frac{q(2d-1)}{d^2 - 1}} L_j[\psi_\theta^{C,(0)}]. \quad (\text{G23})$$

Eq. (G22) and Eq. (G23) show \tilde{J} and \tilde{L} are proportional to their noiseless versions. The same holds when input state is any stabilizer state $U^{C,(i)} |0^{\otimes n}\rangle$. Therefore, for global depolarizing noise, we have

$$X_j(\psi^{C,(i)}; \theta) = \frac{i(d+1)}{2d(1 - q + \frac{q}{d^2 - 1})} [|\psi_\theta^{C,(i)}\rangle \langle \psi_\theta^{C,(i)}|, P_j], \quad (\text{G24})$$

which in the noiseless case (i.e., $q = 0$) equal to Eq. (121). In general, it is difficult to obtain closed-form expressions of deviation observables for random stabilizer states under Pauli noise because $\tilde{J}(\rho_{\text{RP}}^C)$ may not be diagonal.